Chapter 2. PV ELECTRICAL CHARACTERISTICS

Calculating direct-coupled PV output requires a complete description of the current-voltage (1- V) characteristics of the PV array under all operating conditions. In this chapter, five mathematical models of PV current-voltage behavior are analyzed. Theoretical and experimental comparisons are included. Emphasis is given to a "lumped, single mechanism, four parameter" I-V model (hereafter, the acronym "UP" will be used). The term "lumped" refers to the type of approximation, and "single mechanism" refers to the degree of approximation used to model a PV cell with a simplified electrical equivalent circuit. These terms are detailed in Section 2.3.2. Of all of the models compared, the UP model provided the best match with experimental I-V curve data. The UP model was chosen to describe PV system behavior in the final model to estimate long-term direct-coupled PV performance.

2.1 I-V Model Criteria

There are many possible mathematical relationships of varying complexity which can be used to describe PV cmrent-voltage behavior. Depending on the application (in this case, a procedure for estimating long-teml direct-coupled PV performance), several factors need to be considered to assess the suitability of any particular mathematical I-V model.

One is an inherent tradeoff between simplicity and accuracy. A primary goal of this work is to create a reduced set of weather data representing long-term behavior in order to speed calculations and reduce weather data storage requirements. An appropriate

I-V model, then, does not sacrifice this advantage by adding complex or lengthy calculation procedures. However, the I-V model needs to be capable of predicting I-V behavior within the same range of uncertainty as the weather data input to the model.

Another important consideration is whether the data needed to use an I-V model are readily available to the system designer. Models with a large number of parameters, although possibly more accurate, either requires access to generally unpublished and proprietary manufacturer's data, or else require prototype test data. The most detailed, consistent information commonly available is provided in brochures from commercial module manufacturers. Enough information is supplied in such brochures to enable the designer to solve for as many as four parameters at reference test conditions, and enough additional information is ordinarily included to determine how these four parameters vary with temperature and/or solar radiation. Section 2.4 of this chapter details the type of information needed and how it is used to determine up to four unknown parameters.

Other desirable I-V model attributes are more obvious. One is that the model needs to be capable of calculating current, voltage, and power relationships over the entire operating voltage range of the PV array (i.e., not just at the maximum power, open circuit voltage, and short circuit current points). Another is that the model need not be capable of calculating extra information not relevant for this application. For example, transient conditions are not considered in estimating long-term output; therefore, I-V models with transient calculation features are unnecessary. Finally, it is not anticipated that this procedure will be used for sun-concentrating systems.

Therefore, models with fewer parameters than are necessary for concentrating systems are satisfactory for describing I-V curves over ordinary sunlight intensities.

2.2 Overview of I-V Models

Table 2 lists the I-V models evaluated for possible use in the overall direct-coupled modeling method. Acronyms and descriptive keywords used in the table are explained in the following text. Referring to the criteria outlined in Section 2.1, these models were selected because:

- Each has few enough parameters so that the data required to use them can be obtained from widely available PV manufacturers' brochures. Some of the models have more than four parameters, but the additional parameters can have values assigned to them with good accuracy, thereby reducing the number of actual unknowns to four or less.
- Each is useful for steady state calculations only.
- None have additional parameters or high sunlight concentration boundary conditions that attempt to describe concentrated-sun I-V behavior.
- All but the simple linear model for maximum power-tracking systems (as used in programs such as PV f-Chart and PVFORM) are capable of describing complete I-V curves. The simple linear model is widely used and has demonstrated good agreement with experiments for maximum power-tracked systems [21,22]. Therefore, it is used as a measure of comparison for the other

I-V models, but only at the predicted maximum power point. At a minimum, an I-V model must satisfactorily predict the maximum power point (as well as other points on the full I-V curve).

Table 2. I-V Curve Models

Acronym	Model Description
2M6P	Lumped, 2 Mechanism model with 6 Parameters
2M5P	Lumped, 2 Mechanism model with 5 Parameters
L4P	Lumped, 1 Mechanism model with 4 Parameters
L3P	Lumped, 1 Mechanism model with 3 Parameters
MIT	Mass. Inst. of Tech. model, developed by TRW Corp.; a hybrid between the L4P and L3P models; used in TRNSYS/MIT and also by New Mexico Solar Energy Inst.
LINEAR	Simple linear model for calculating maximum power output only; used in PV f-Chart, PVFORM, and other simplified programs.

2.3 PV Electrical Equivalent Circuits

As mentioned in the introductory chapter, it is beyond the scope of this study to explain the complex microscopic phenomena of how charges are created separated, and collected in a PV circuit A macroscopic mathematical description of these phenomena is of interest. however. In this section, PV electrical equivalent circuits and their conesponding equations are shown for each of the I-V curve models listed in Table 2. Basic equations governing PV device behavior are explained fIrst, followed by a

sequence of generalized equivalent circuits. The generalized circuits are too complex to be used for a system design procedure, but they provide a starting point from which the models in Table 2 are derived after various simplifications. In the following sections of this chapter, dIe models in Table 2 are compared in more detail.

2.3.1 Basic Equivalent Circuits and I-V Relations

To develop an accurate equivalent circuit for a PV cell, it is necessary to understand the physical configuration of the elements of the cell as well as the electrical characteristics of each element. Figure 3 is a cross-sectional view showing major components of a typical PV cell.

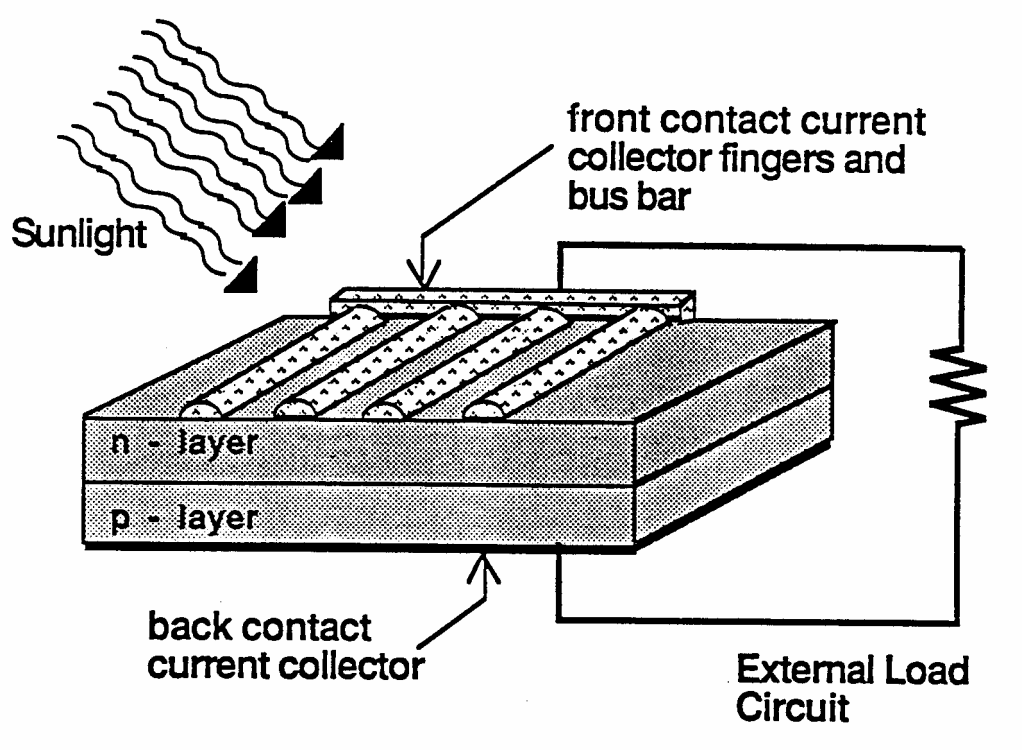

Figure 3. PV Cell Schematic

The junction of the dissimilar *n* (net negative charge) and *p* (net positive charge) layers creates a diode effect. When illuminated the layers act simultaneously as a constant current source in parallel with the diode. These basic PV circuit elements are depicted in the simple (two parameter) ideal equivalent circuit of Figure 4. An important feature of this circuit is that it is assumed there is a single, or lumped, mechanism by which current is generated from absorbed light and a single mechanism by which this current can be shunted across the load rather than flow through it.

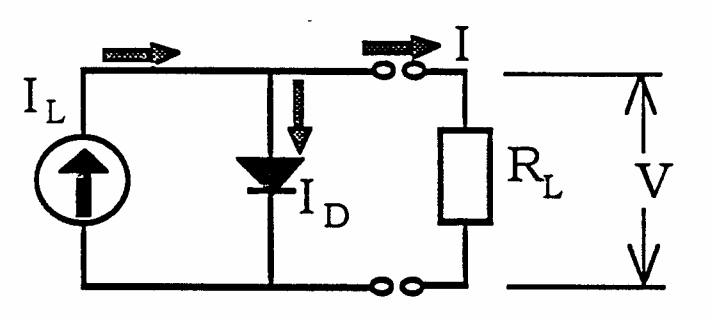

Figure 4. Ideal PV Cell Equivalent Circuit

A nodal current balance, with assumed current directions as shown, yields the following expression:

$$I = I_L - I_D \tag{2.1}$$

I = output current

V = output voltage

R_L = load impedance (for an unspecified load type)

I_L = light-generated current = *f*(irradiance, cell temperature, material, area)

I_D = diode, or junction, current = *f*(V, cell temperature, and material)

The light current is, to a very good approximation, directly proportional to the intensity of absorbed solar radiation. The light current is linearly related to cell temperature, and is also dependant on the materials used and fabrication processes. For a given cell, the light current is conveniently expressed relative to that measured for the same cell at a reference irradiance, usually 1000 Watts per square meter, and a reference cell temperature, usually about 298 K:

$$I_L = \left(\frac{\Phi}{\Phi_{REF}} \right) \times (I_{L,REF} + \mu_{ISC} \times (T_C - T_{C,REF})) \qquad (2.2)$$

Φ, Φ_{REF} = irradiance at the new and reference conditions, W/m^2.

$I_{L,REF}$ = light current, in amps, at the reference condition.

μ_{ISC} = Manufacturer-supplied temperature coefficient of short circuit current in amps per degree. (As will be shown later, the short circuit current is nearly identical to the light current. For practical purposes, the terms are interchangeable).

$T_C, T_{C,REF}$ = cell temperature at the new and reference conditions.

The diode current is calculated as:

$$I_D = I_O \times (\exp\left(\frac{qV}{\gamma k T_C} \right) - 1) \qquad (2.3)$$

I_O = reverse saturation current =.f(T co material)

q = electron charge constant, 1.602 x $l0^{-19}$ C

k = Boltzmann constant, 1.381 x $l0^{-23}$ J/K

γ = completion, or shape, factor, A (A = 1.0 for an ideal cell), multiplied by the number of cells wired in series, NCS (also 1 in this example). The completion factor is a measure of cellular imperfection and is not directly measurable.

The reverse saturation current, in turn, is:

$$I_O = D \times (T_C)^3 \times \exp\left(\frac{q\varepsilon_G}{AkT_C} \right) \qquad (2.4)$$

D = diode diffusion factor, approximately constant.

ε_G = material bandgap energy (1.12 eV for Si, 1.35 eV for GaAs).

The other terms are as defined above for Eqn. 2.3. For the ideal cell, the two

unknown parameters are I_L and I_O. The functional relationships for I_L (Eqn. 2.2) and I_O (Eqn. 2.4) with respect to changes in irradiance and cell temperature apply to all subsequent equivalent circuits, except for the MIT model. Additional simplifying assumptions are used in the MIT model as well as different algebraic groupings of the various parameters and constant terms. Consequently, different relationships are employed to track variations in the I-V characteristic with changes in irradiance and temperature. The actual equations used in the MIT model are detailed in Section 2.3.3.5.

The diode current In creates the characteristic I-V curve shape of the PV cell. Adding the light current translates the curve upwards. Figure 5 shows both the diode I-V curve and the overall cell I-V curve for an ideal cell with assumed current directions as shown in Figure 4, power is generated only in the first quadrant. The I-V equation can be extended into the second or fourth quadrants. but in those regions the cell is absorbing energy.

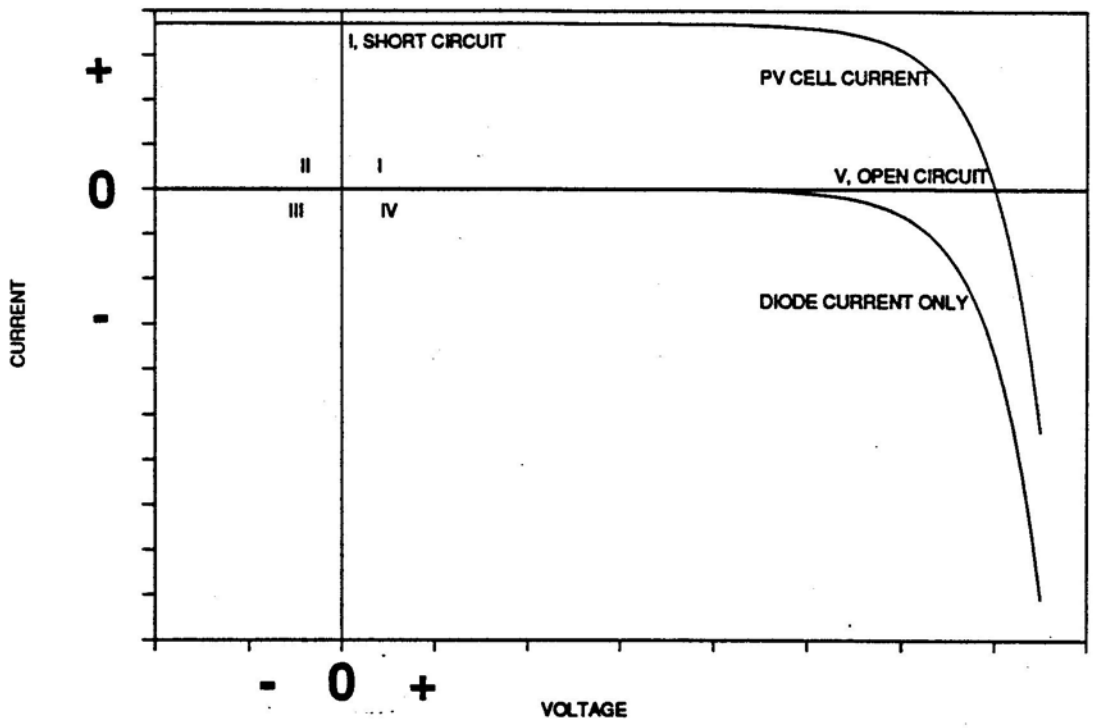

Figure 5. Cell and Diode I-V Curves for Ideal PV Cell

2.3.2 Generalized Equivalent Circuits

In an actual cell (or module or array) other structural imperfections and inherent material properties introduce resistances and other inefficiencies which limit the device output. Also, light currents and diode currents within an actual cell are not created at single "1umped" elements as indicated in Figure 4. Rather, they are distributed over the cell volume. Likewise, current collection is distributed over the top and bottom faces. There are greater losses on the top surface due to oppositely charged carriers recombining before the desired charges can migrate to a finger on the collector grid. An optimal tradeoff exists between improving the current collection efficiency by increasing the collector grid area and increasing the absorbed radiation by reducing the grid area.

2.3.2.1 Distributed Equivalent Circuit

A generalized equivalent circuit which better approximates the distributed nature of the PV cell and its various loss mechanisms is shown in Figure 6. Equations for the individual circuit elements are of the same form as those used to describe the simple circuit in Figure 4, but there are more of them (for example, "n" diode current equations), and the voltage argument in the exponential term of each diode equation (Eqn. 2.3) is much more complex. Instead of using output voltage V in Eqn 2.3. the voltage argument for each of the n diodes is a lengthy expression which accounts for voltage drops across each resistance between that diode and the output terminal. In the limit as n $\rightarrow\infty$, the corresponding I-V expression is a differential equation.

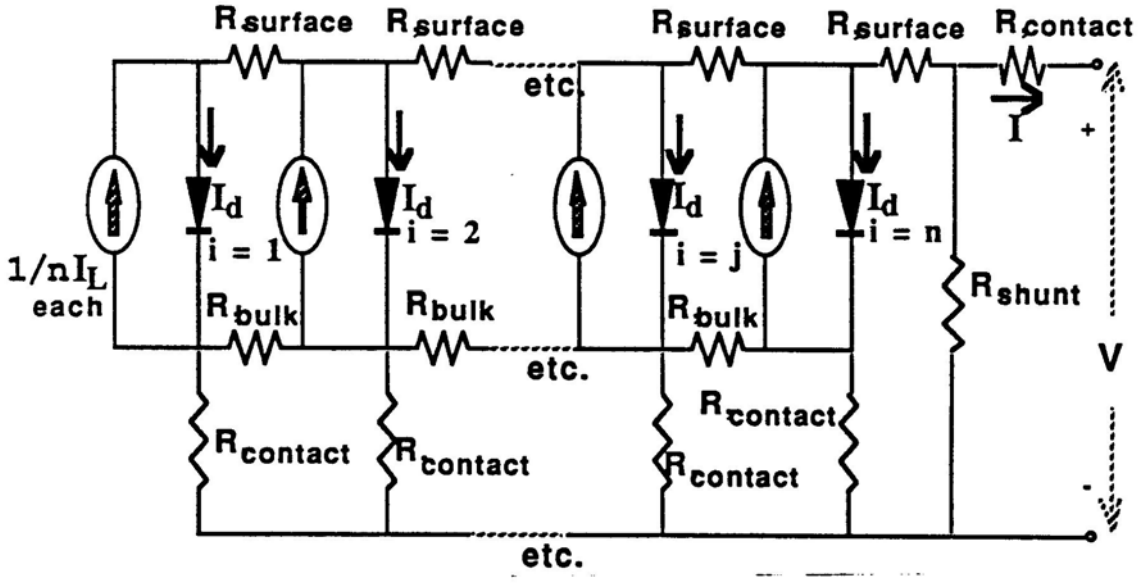

Figure 6. Distributed Equivalent Circuit

The above circuit is nearly identical to that described by Wolf [23] in 1961, except that it has been further generalized to include a shunt resistance component often

found in the literature (e.g., Sze [2], Pfeiffer et aI. [4], Kreith and Kreider [24], Rosenblum [25]). Even without the shunt resistance t~ Wolf concluded that such a circuit was far too complex to evaluate, i.e., to obtain practical expressions for I and V at the output terminals. Furthermore, Wolf concluded that, (even in 1961 vintage cells), the internal resistances of "modem" cells were too small to warrant such a detailed treatment. An exception occurs when highly concentrated solar radiation is used, as shown by Pfeiffer, et al. [4].

2.3.2.2 Wolf's Improved Lumped Equivalent Circuit

In the same article, Wolf [23] also observed that approximating the distributed cell by dividing the cell into many separate diode and current source mechanisms was unnecessary. He demonstrated excellent agreement with experimental I-V curves using the (somewhat) simpler seven parameter equivalent circuit shown in Figure 7. As an approximation to a distributed circuit, this circuit includes two pairs of similar (four total) lumped diodes and two lumped current source mechanisms. There are two lumped series resistance mechanisms. one representing the combined lumped effect of upper and lower contact series resistance, bulk series resistance, and a portion of the surface series resistance, and the other representing the remaining surface series resistance.

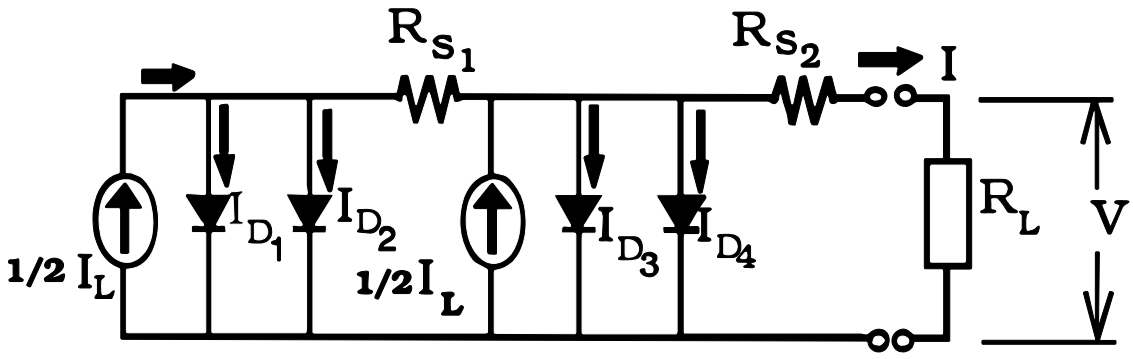

Figure 7. Wolf's Improved Lumped Equivalent Circuit

The I-V equation describing this circuit is:

$$I = \frac{1}{2} I_L - I_{D1} - I_{D2} + \frac{1}{2} I_L - I_{D3} - I_{D4} \tag{2.5}$$

$$I_{D4} = I_{O2} \times \left(\exp\left(\frac{q}{A_2 k T_C} \left(V + I R_{S2} \right) \right) - 1 \right) \tag{2.6}$$

$$I_{D3} = I_{O1} \times \left(\exp\left(\frac{q}{A_1 k T_C} \right) \left(V + I R_{S2} \right) - 1 \right) \tag{2.7}$$

$$I_{D2} = I_{O2} \times \left(\exp\left(\frac{qV}{A_2 k T_C} \times \left(V + I R_{S2} \left(I - \frac{1}{2} I_L + I_{D3} + I_{D4} \right) R_{S1} \right) \right) - 1 \right) \tag{2.8}$$

$$I_{D1} = I_{O1} \times \left(\exp\left(\frac{qV}{A_1 k T_C} \times \left(V + I R_{S2} \left(I - \frac{1}{2} I_L + I_{D3} + I_{D4} \right) R_{S1} \right) \right) - 1 \right) \tag{2.9}$$

The parameters for this circuit are:

I_L = light current, distributed evenly over the two mechanisms

I_{O1} = reverse saturation current (same for diodes 1 and 3)

I_{O2} = reverse saturation current (same for diodes 2 and 4)

A_1 = completion factor = 1.0 (same for diodes 1 and 3)

A_2 = completion factor> 1.0 (same for diodes 2 and 4)

R_{S1} = contact, bulk, and partial surface series resistance

R_{S2} = remaining surface series resistance

The other terms are as defined previously. Note that one parameter, A_1, 1.0, and therefore diodes 1 and 3 are assumed to exhibit ideal behavior. The result of this assumption is that the quantities I_{D3} and I_{D4} only become large near the cell's open circuit voltage, where cells have been observed to exhibit near-ideal behavior [23]. A_2, the completion factor associated with the other diode currents, is intended to model non-ideal

diode behavior, It is greater than 1.0 and is the dominant term at low voltages. Although by definition this is a seven parameter mode, it reduces to a six parameter model when A_1 is fixed beforehand. In practice, one would need to know I and V at six points, write Eqn. 2.5 six times, and solve the 6 x 6 set of simultaneous independent equations for the unknown parameters.

2.3.2.3 Dual Lumped Parameter Equivalent Circuit

The two previous generalized equivalent circuits have been outlined mainly to show the fundamental forms from which simpler equivalent circuits may be derived.

The dual lumped parameter circuit shown in Figure 8 is a simplified version of the distributed circuit, Figure 6, borrowing from ideas advanced in Wolf's lumped circuit, Figure 7 [23]. With seven parameters, it is also too complex to be used for this study.

However, there are two principal reasons why it is explained in more detail in the text which follows. One is that the I-V models which are selected for detailed comparison later in this chapter are readily derived from this "parent" model; it therefore provides a common basis for comments when model features are compared. The other reason is that, as with Wolf's model, the actual number of parameters that need to be calculated can be reduced if some of them can be arbitrarily chosen with good accuracy beforehand and treated as known quantities. The potential advantages of doing so will be more apparent upon examining the form of the resulting I-V equations.

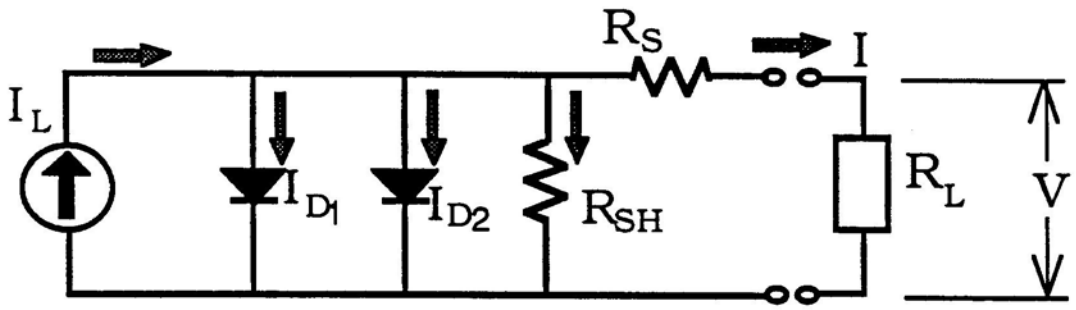

Figure 8. Dual Lumped Parameter Equivalent Circuit

The I-V equation describing this circuit is:

$$I = I_L - I_{D1} - I_{D2} - \frac{(V + IR_S)}{R_{SH}} \tag{2.10}$$

$$I_{D1} = I_{O1}\left(\exp\left(\frac{q}{\gamma_1 kT_C} \times (V + IR_S) \right) - 1 \right) \tag{2.11}$$

$$I_{D2} = I_{O2}\left(\exp\left(\frac{q}{\gamma_2 kT_C} \times (V + IR_S) \right) - 1 \right) \tag{2.12}$$

Substituting Eqns. 2.11 and 2.12 into 2.10 and rearranging gives:

$$I = \left[I_L - I_{O1}\left(\exp\left(\frac{q(V + IR_S)}{\gamma_1 kT_C} \right) - 1 \right) - I_{O2}\left(\exp\left(\frac{q(V + IR_S)}{\gamma_2 kT_C} \right) - 1 \right) - \frac{V}{R_{SH}} \right] \times \left[\frac{R_{SH}}{R_S + R_{SH}} \right] \tag{2.13}$$

The parameters for this circuit are:

I_L = light current

I_{01} = reverse saturation current

I_{02} = reverse saturation current

$\gamma_1 = A_1$ x (NCS)

$\gamma_2 = A_2$ x (NCS)

NCS = number of cells in series

R_S = apparent lumped series resistance

R_{SH} = apparent lumped shunt resistance

The other terms are as defined previously. As with Wolf's lumped circuit, A_1 is set to 1.0, leaving six unknown parameters. Equation 2.13 reduces to Equation 2.1, the ideal two parameter lumped equivalent circuit, when I_{01} and R_S equal zero, A_2 equals 1.0, and R_{SH} is infinite.

2.3.3 Simplified Equivalent Circuits

Using the dual lumped parameter circuit as a starting point, the circuits and equations corresponding to the I-V models in Table 2 can be derived by making successive simplifications.

The first simplification made to the dual lumped parameter circuit of Figure 8 is common to each of the simplified equivalent circuits which follow. This simplification assumes the shunt resistance is infinite and therefore the shunt current is negligible.

This simplification is justified by the fact that the shunt resistance is ordinarily much larger than other resistances, and only affects the I-V curve shape significantly if the irradiance is extremely low. Even then, the effect on the curve shape is not important at low voltages. At higher voltages, the output current is progressively lowered due to an increasing shunt current, the I-V curve "shrinks," an4 the open circuit voltage is

decreased. Assuming infinite shunt resistance introduces little error in long-term output estimates since the potential electricity produced at low light levels is small.

A comparison of the effect of shunt resistance on modeled I-V behavior is illustrated in Figures 9 and 10 for a typical module, at irradiance levels of 1030 W/m^2 and 125 W/m^2. At 1030 W/m^2, the differences between the two I-V curves are barely perceptible. One curve assumes infinite shunt resistance while the other assumes a shunt resistance of 500 ohms. The difference in maximum power output for these two curves is about 0.6%. For the lower irradiance shown in Figure 10, the differences in the two I-V curves are more pronounced, and the difference in maximum power output is about 4.5%. However, the effect of this difference is small because the irradiance, and thus the generated power, is low. The SOO ohm shunt resistance is much smaller than normally measured and was chosen to exaggerate differences in the I-V shape. A typical value for modules of this size is about 60 million ohms [26]. The series resistance, by comparison, is only about 0.2 ohms.

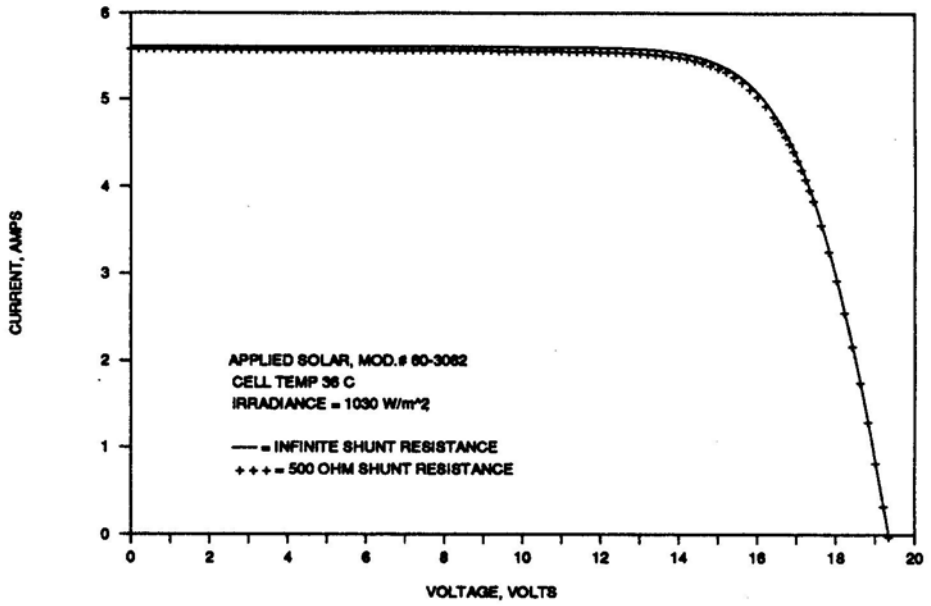

Figure 9. Effect of Shunt Resistance at High Irradiance

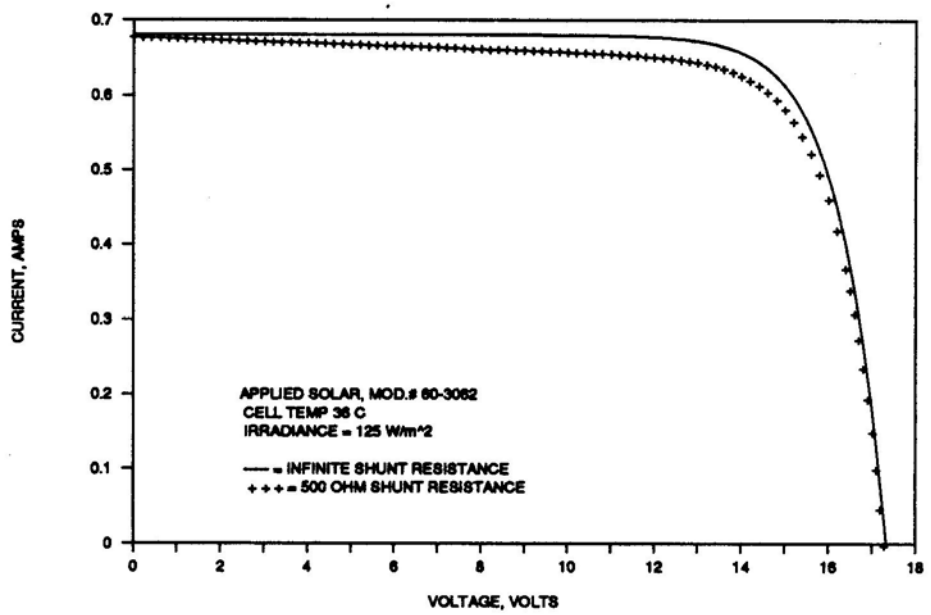

Figure 10. Effect of Shunt Resistance at Low Irradiance

Another partial justification for assuming infinite shunt resistance is that shunt currents are not an inherent loss mechanism dictated by material properties, the way bulk series resistance is, for example. Shunt currents are principally due to current leakage along edges and comers of the cell, and these effects are minimized by constructing the module within a framework of good electrical insulators [24].

2.3.3.1 Lumped, 2 Mechanism, 6 Parameter Equivalent Circuit

The first I-V model evaluated for use in the long-term performance estimating procedure is based on the equivalent circuit shown in Figure 11. This will be referred to as model "2M6P." This circuit is derived from the "parent" circuit of Figure 8 by making one simplification. The simplification results from assuming the shunt resistance is so large that the current path through it is negligible, as explained in the preceding section.

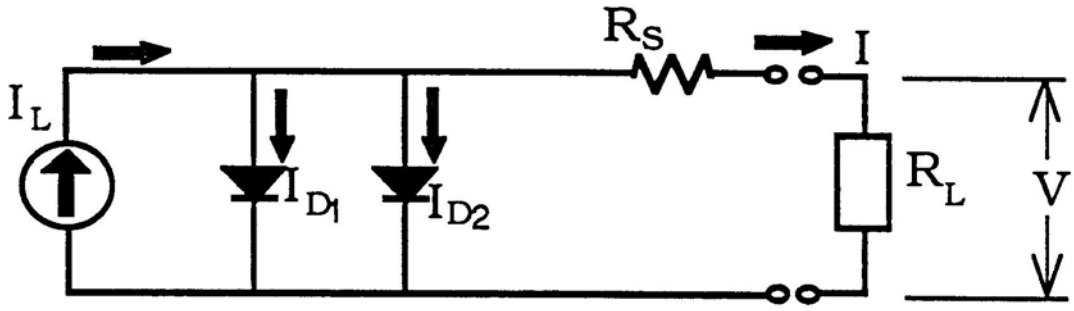

Figure 11. Two Mechanism, Six Parameter Equivalent Circuit

The current-voltage relationships for this circuit are as follows:

$$I = I_L - I_{D1} - I_{D2} \tag{2.14}$$

$$I_{D1} = I_{O1}\left(\exp\left(\frac{q}{\gamma_1 kT_C}\times\left(V + IR_S\right)\right) - 1\right) \tag{2.15}$$

$$I_{D2} = I_{O2}\left(\exp\left(\frac{q}{\gamma_2 kT_C}\times\left(V + IR_S\right)\right) - 1\right) \tag{2.16}$$

Substituting Eqns. 2.15 and 2.16 into 2.14 gives:

$$I = I_L - I_{O1}\left(\exp\left(\frac{q\left(V + IR_S\right)}{\gamma_1 kT_C}\right) - 1\right) - I_{O2}\left(\exp\left(\frac{q\left(V + IR_S\right)}{\gamma_2 kT_C}\right) - 1\right) \tag{2.17}$$

The six parameters for this circuit are:

I_L = light current

I_{01} = reverse saturation current

I_{02} = reverse saturation current

$\gamma_1 = A_1$ x (NCS)

$\gamma_2 = A_2$ x (NCS)

R_S = series resistance

It was asserted earlier that a maximum of four parameters can be determined from manufacturer-supplied information (an explanation of this limit is given in Section 2.4.3). In order to use this relatively complex equation, two parameters can be assigned values and treated as known quantities. As with Wolf's lumped circuit, A1 is set to 1.0. The second arbitrarily assigned parameter, ~, is set to 2.0, based on an analysis by Sah, Noyce, and Shockley [27] and discussed by Loferski in a 1972 National Academy of Sciences report [28]. The number of cells in series, NCS, is a known quantity selected by the designer.

2.3.3.2 Lumped, 2 Mechanism, 5 Parameter Equivalent Circuit

The "2M5P" equivalent circuit is obtained by making one additional simplification to the "2M6P" circuit shown in Figure 11. For the 2M5P circuit, it is assumed that the series resistance is negligible. With zero series resistance, the equivalent circuit reduces to the form shown in Figure 12.

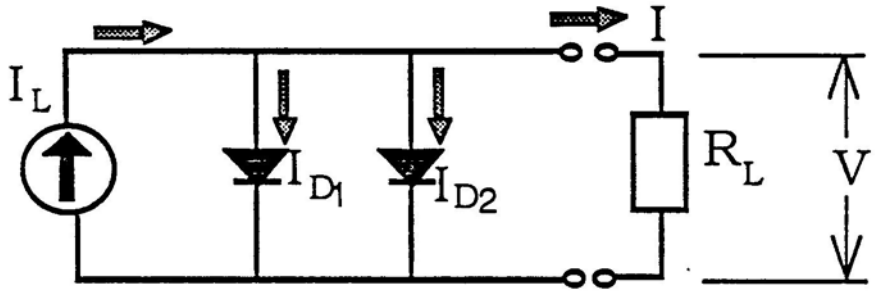

Figure 12. Two Mechanism, Five Parameter Equivalent Circuit

The current-voltage relationships for this circuit are as follows:

$$I = I_L - I_{D1} - I_{D2} \tag{2.18}$$

$$I_{D1} = I_{O1}\left(\exp\left(\frac{qV}{\gamma_1 kT_C}\right) - 1\right) \tag{2.19}$$

$$I_{D2} = I_{O2}\left(\exp\left(\frac{qV}{\gamma_2 kT_C}\right) - 1\right) \tag{2.20}$$

Substituting Eqns. 2.19 and 2.20 into 2.18 gives:

$$I = I_L - I_{O1}\left(\exp\left(\frac{qV}{\gamma_1 kT_C}\right) - 1\right) - I_{O2}\left(\exp\left(\frac{qV}{\gamma_2 kT_C}\right) - 1\right) \tag{2.21}$$

The five parameters for this circuit are:

I_L = light current

$\gamma 2$ = reverse saturation current

I_{02} = reverse saturation current

$\gamma_1 = A_1$ x (NCS)

$\gamma_2 = A_2$ x (NCS)

2.3.3.3 Lumped, 1 Mechanism, 4 Parameter Equivalent Circuit

This circuit is obtained from the "parent" dual lumped parameter circuit shown in Figure 8 by making the following assumptions. First, as with the two previous simplified circuits, the shunt resistance is assumed to be infinite. Then, it is assumed that one lumped diode mechanism can be used to represent the overall diode characteristics of the cell. The resulting equivalent circuit, which will be referred to as the "UP" circuit, is shown in Figure 13.

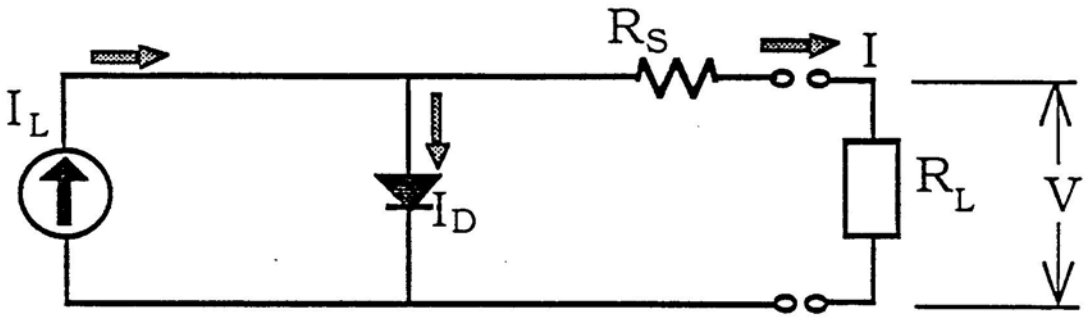

Figure 13. Single Mechanism, Four Parameter Equivalent Circuit

The current-voltage relationships for this circuit are as follows:

$$I = I_L - I_D \tag{2.22}$$

$$I_D = I_O\left(\exp\left(\frac{q}{\gamma kT_C}\times\left(V + IR_S\right)\right) - 1\right) \tag{2.23}$$

Substituting Eqns. 2.23 into 2.22 gives:

$$I = I_L - I_{O1}\left(\exp\left(\frac{q}{\gamma kT_C}\times\left(V + IR_S\right)\right) - 1\right) \tag{2.24}$$

The four parameters for this circuit are:

I_L = light current

I_0 = reverse saturation current

γ = A x (NCS)

R_S = series resistance

For this circuit, it is not necessary to assign arbitrary values to any of the parameters since they can be determined from information provided by manufacturers.

2.3.3.4 Lumped, 1 Mechanism, 3 Parameter Equivalent Circuit

If the series resistance is assumed to be zero (as was done for the 2M5P circuit) the UP circuit reduces to the three parameter circuit shown in Figure 14. This equivalent circuit is identical to the ideal circuit shown in Figure 4t except that" At" the completion factor, is treated as an unknown in order to describe non-ideal diode behavior (i.e., A ≠ 1.0),

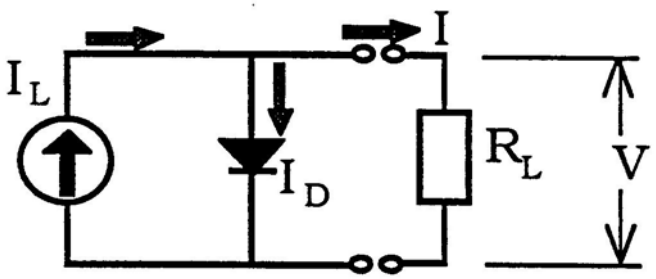

Figure 14. Single Mechanism Three Parameter Equivalent Circuit

The current-voltage relationships for this circuit are as follows:

$$I = I_L - I_D \tag{2.25}$$

$$I_D = I_O\left(\exp\left(\frac{q}{\gamma kT_C}\right)-1\right) \tag{2.26}$$

Substituting Eqns. 2.26 into 2.25 gives:

$$I = I_L - I_O\left(\exp\left(\frac{qV}{\gamma kT_C}\right)-1\right) \tag{2.27}$$

The three parameters for this circuit are:

I_L = light current

I_0 = reverse saturation current

γ = A x (NCS)

As with the UP circuit, it is not necessary to assign arbitrary values to any of the parameters.

2.3.3.5 MIT I-V Model Equivalent Circuit

The MIT model equivalent circuit is a hybrid between the L3P and L4P circuits. Like the L3P and UP circuits, it uses a single lumped mechanism for current generation and also for the diode current. This model is viewed as a hybrid because the series resistance is neglected at an initial reference condition to obtain three unknown parameters, as in the L3P model, but is included when calculating new parameter values for I-V curves at other conditions, as in the UP model [29]. The MIT I-V equation requires the user to treat the series resistance as a known quantity rather than solve for it as one of the unknown parameters. Lastly, the MIT model requires one additional piece of information not explicitly needed by the previous models, μ_{voc}. μ_{voc} is the temperature coefficient of open circuit voltage (V /K) and is usually given by the module manufacturer.

This model is more difficult to compare side by side with the previous models because of a difference in the way the I-V characteristic is calculated. In each of the

previous simplified models, the parameters ~ and lo are recalculated at off-reference conditions based on the irradiance and cell temperature auxiliary relationships outlined in Section 2.3.1. All other parameters are assumed constant once they are solved for at a reference condition. The result is a new I-V equation which yields current as a function of voltage only.

The MIT model, although the terms in the I-V equation look different, is only an algebraic rearrangement of the I-V equation used for the simple three parameter model. In particular, the open circuit voltage, $V_{OC'}$ is an explicit parameter in the MIT equation, but not in the I-V equations for the other models. Also, the term I_{SC} is used in place of I_L, but as stated in Section 2.3.1, for all practical purposes these terms are interchangeable. Actually, for a cell model which assumes zero series resistance, the terms are equivalent.

The important difference between the MIT model and the previous I-V models is in the way the I-V curve is calculated at irradiances and cell temperatures differing from the reference condition. The series resistance is not an explicit parameter in the I-V equation. Rather, it is used only in an auxiliary equation to calculate variations in the open circuit voltage. Also, a comparison of I-V Eqns. 2.28 and 2.27 shows that the reverse saturation current, 100 is replaced in the MIT circuit by the product of I_{SC} and constant C_1. This regrouping forces the diode current to be a function of irradiance in the MIT circuit, which is incorrect. Diode behavior is the same under dark or illuminated conditions. To use the MIT equation at conditions other than the reference conditions, it is necessary to recalculate V_{OC} and I_{SC} instead of I_O and I_L. The MIT I-V equation,

related auxiliary equations, and a procedure to calculate I_{SC} and V_{OC} at any condition follow.

$$I = I_{SC}\left[1 - C_1\left(\exp\left(\frac{V}{C_2 V_{OC}}\right) - 1\right)\right] \tag{2.28}$$

where the constants C_1 and C_2 are:

$$C_1 = \left(1 - \frac{I_{MP}}{I_{SC}}\right)\exp\left(\frac{= V_{MP}}{C_2 V_{OC}}\right) \tag{2.29}$$

$$C_2 = \frac{\frac{V_{MP}}{V_{OC}} - 1}{\ln\left(1 - \frac{I_{MP}}{I_{SC}}\right)} \tag{2.30}$$

Constants C_1 and C_2 are not independent. The other new terms are supplied by the manufacturer:

V_{MP} = Maximum power point voltage at reference conditions.

I_{MP} = Maximum power point current at reference conditions.

A set of auxiliary translation equations is used to either recalculate the I-V equation at new conditions, or to translate any I-V point on one curve to a new I-V coordinate at new conditions.

$$I_{NEW} = I_{REF} + \Delta I \tag{2.31}$$

$$V_{NEW} = V_{REF} + \Delta V \tag{2.32}$$

$$\Delta T = T_C - T_{C,REF} \tag{2.33}$$

$$\Delta I = I_{SC,REF}\left(\frac{\Phi}{\Phi_{REF}} - 1\right) + \mu_{ISC}\left(\frac{\Phi}{\Phi_{REF}}\right)\Delta T \qquad (2.34)$$

$$\Delta V = \mu_{VOC}\Delta T - R_S\Delta I \qquad (2.35)$$

μ_{VOC} = Manufacturer-supplied temperature coefficient of voltage, in units of Volts/C. The other terms have been defined previously.

When recalculating the I-V equation under new conditions, the only parameters that need to be updated are I_{SC} and $V_{OC'}$ as C_1 and C_2 are assumed constant. I_{SC} is updated using Equations 2.31, 2.33, and 2.34. Voc is updated using the following procedure:

1. A new V_{OC} is the result of a translation, or mapping, of an unknown I-V point on the old, or reference, I-V curve. The I-V coordinates of this "old" point must be determined first. I_{NEW} is zero at the new $V_{OC'}$ Eqn. 2.31 shows, by inspection, that I_{REF} must equal -ΔI.

2. ΔI is calculated using Eqn. 2.34. I_{REF} is now known.

3. The V coordinate of V_{REF} corresponding to I_{REF} is found from the original I-V equation, Eqn. 2.28, evaluated at I = I_{REF}

4. The translation ΔV is calculated with Eqn. 2.35.

5. The new V_{OC} is found with Eqn. 2.32.

Once V_{OC} and I_{SC} are updated, the result is a new I-V equation valid at the new irradiance and cell temperature.

2.3.3.6 Linear Maximum Power Model

As stated in Section 2.2, the simple linear model is not able to describe full I-V curves. It is intended for calculating maximum power point output as a function of irradiance, cell temperature, and reference condition array data. Less information about the PV system is needed to use it than any of the complete I-V curve models. Although less versatile than other models, it is accurate and widely used in programs which estimate performance for maximum power-tracked systems [11,12,13]. For this reason, it is used to provide a measure of comparison to the other I-V models' predicted maximum power output, along with experimental maximum power point data from Pacific Gas and Electric Company [30] and the New Mexico Solar Energy Institute [31].

The equation used to calculate maximum power point output, in Watts, is:

$$P_{MAX} = \frac{\Phi}{\Phi_{REF}} P_{MAX,REF}\left(1 - \beta\left(T_C - T_{C,REF}\right)\right) \qquad (2.36)$$

β = Manufacturer-supplied temperature coefficient of maximum power, 1/C.

PMAX, PMAX,REF = Maximum power output at new and reference conditions, W.

2.4 Solving I-V Equations

The previous sections in this chapter have outlined several equivalent circuits and their accompanying mathematical descriptions. Several comments have been made about the number of unknown parameters in each I-V equation. The following subsections address how to determine the parameters and create workable I-V equations by setting up and solving systems of simultaneous non-linear equations in several unknowns. Some of

the parameters can be determined using manufacturer-supply information, while others may need to be specified by the user. Once values for each parameter are calculated (or in some cases, chosen), the resultant I-V equation gives a continuous analytical expression of current as a function of voltage, at a reference irradiance and cell temperature. At other irradiances and cell temperatures, some of the parameters vary, and auxiliary equations are needed to calculate updated values at each set of conditions. The updated parameters yield a new I-V equation valid under the new conditions.

2.4.1 Overview of Solution Methods

The solution methods for each of the five simplified I-V models introduced in the previous Sections 2.3.3.1 thru 2.3.3.5 are similar. Only one of these, the UP model, is examined in detail, because a side by side evaluation relative to experimental data (Section 2.8) showed this to be the most appropriate model to use within the long-term performance estimating model. Although a stepwise solution method was not shown, the MIT model was presented in Section 2.3.3.5 in a "solved" form; that is, each unknown term had already been solved for in terms of known quantities picked from manufacturer's data. The same is true for the LINEAR model (Section 2.3.3.6); its two parameters can be "solved" by inspection using data obtained from the manufacturer.

The basic approach to solving for the unknown quantities in I-V equations is to consider what information is normally published by PV manufacturers and how that information can be used to help predict I-V behavior under varying conditions. The most important information needed from the manufacturer are the module short circuit current,

open circuit voltage, and maximum power point current and voltage, all measured at the same reference irradiance and cell temperature. This information fixes three I-V points, all of which must lie on the same I-V curve and therefore, satisfy the same I-V equation.

The three data points on the I-V curve permit three independent versions of the I-V equation to be written. The result is a non-linear system of three simultaneous equations, which can be solved for three unknowns. Depending on which I-V equation is being used, the 3 x 3 system can in some instances be solved explicitly by simple substitution, or in general, can be solved numerically.

For the L3P circuit, the three unknowns are the light current, I_L, the reverse saturation current I_O, and the curve-fit factor, y. For the 2M5P circuit with A_1 and A_2 set equal to 1 and 2, respectively, the three remaining unknowns are ~ and the two reverse saturation currents, I_{01} and I_{02}. The 2M6P and UP circuits cannot be solved in this manner because there is a fourth unknown, the apparent series resistance, R_S (i.e., the lumped effect of distributed series resistance loss mechanisms). Solving for the series resistance parameter is addressed in the following section.

2.4.2 The Series Resistance Parameter

The series resistance term proves to be an important parameter, especially for irradiances and cell temperatures far from the reference condition. Given the same set of reference conditions, each I-V model traces I-V curves that are very similar - but only near the reference conditions. Away from the reference conditions, I-V models which

include a series resistance term describe I-V curves that are quite different than the curves described by models which neglect series resistance. Over a full range of operating conditions, such as in an annual simulation, the predicted output (for maximum power-tracked systems) when series resistance is neglected ranges from 5 to 8% *lower* than if the "correct" series resistance is used This will be demonstrated in more detail in Section 2.8.

In this section, five methods of determining series resistance are compared. In methods 1,2,4, and 5, estimating the series resistance is prerequisite to solving for the remaining three parameters in a 3 x 3 system of equations. Method 3 is more complex, because a 4 x 4 system is solved simultaneously. In decreasing order of preference, they are:

Method 1. Use the manufacturer's stated value. This reduces the problem to solving a 3 x 3 system. The drawback is that PV manufacturers do not often publish this quantity.

Method 2. Begin with an assumed value for R, to reduce the number of unknowns to three, and solve the resulting 3 x 3 system. Then, from the "solved" I-V equation, derive an analytical expression for the change in open circuit voltage with respect to temperature (at constant irradiance), $\partial V_{OC}/\partial T_C=\mu_{VOC}$. This analytically calculated value is compared to the manufacturer's estimate for $\mu_{VOC,}$ which is usually given. The process is repeated with new guesses for R, until the measured and derived values for μ_{VOC} match. This method is explained in detail in Section 2.4.5.

Method 3. Generate a fourth independent equation and solve for the series resistance and

other parameters using a 4 x 4 system of equations. The fourth equation results from differentiating the power (I(V) x V) with respect to voltage. At the maximum power point this quantity must equal zero (Figure 2 in Section 1.2). The first three I-V expressions constrain the Iw-V pair, the short circuit, and open circuit points to lie on the same curve. The fourth equation constrains the ~- V w pair to also be the maximum power point on the curve. This method is detailed in Section 2.4.3.

Method 4. If R_S is known for one system, R_S for another may be estimated by scaling R_S for the known system up or down based on the relative magnitudes of the maximum power currents and voltages of the two systems. Series resistance is proportional to voltage and inversely proportional to current.

$$R_{S,NEW} = R_{S,KNOWN}\left[\frac{V_{MP,NEW}}{V_{MP,KNOWN}}\right]\left[\frac{I_{MP,KNOWN}}{I_{MP,NEW}}\right] \qquad (2.37)$$

This type of approximation ignores differences in materials and fabrication and does not scale as well for systems which differ widely in size.

Method 5. Some sources, including the New Mexico Solar Energy Institute [31], MIT [32], and NASA's Lewis Research Center [33], estimate the series resistance by measuring the slope of a sample I-V curve at the open circuit voltage point, and then take the negative reciprocal of the slope. Sample I-V curves are not always given in manufacturers brochures, and when they are provided, the resolution is usually too poor to get a good estimate of the slope. It will be shown shortly that, even when measured accurately, the resulting series resistance estimate will always be too high.

Both the second and third methods attempt to relate the basic I-V equation to

empirical quantities via an additional independent equation. In the second method, the additional equation is used to match the analytical and observed temperature coefficient of open circuit voltage. In the third method, the additional equation is used to match the analytical and observed maximum power point coordinates. Ideally, both of these methods (as well as the other methods) would yield the same result for R_S, but they do not.

A comparison of the calculated R_S values by these various methods is shown in Table 3. Where necessary, the UP I-V model was used as a basis for the calculations. These results show the second (iterative) method to produce generally more consistent results than the third method, which uses the maximum power point constraint. The iterative method consistently predicts a value close to the alternate methods, shown in the last column. Each of the "slope at V_{OC}" measurements were made by the New Mexico Solar Energy Institute (NMSEI) on existing arrays, and were done by "eyeballing" the slope from a printed version of a sample I-V curve. For all but one system, the "slope at V_{OC}" method predicts a higher value than the iterative method; this one aberration may be due to inconsistent data or slope estimating error.

Table 3. Series Resistance Estimates for Nine PV Systems

#	System Description	R_S, ohms, solved by:		
		Method 2. Iterating on μ_{VOC}	Method 3. Constraining $\partial P/\partial V_{MP}=0$	Either: Method 1, given by mfg.; Method 4, scaled; or Method 5, estimated from sample I-V slope at V_{OC}
1	Kyocera 44 W module	0.31	-0.05	0.46 – Method 4 (using data from system #8)
2	Mobil 30 W module	0.74	-0.75	<1.0 – from mfg.
3	Solarex 30 W module	0.57	-0.23	0.79 – Method 4 (using data from system #8)
4	Mobil 720 W array	10.14	-6.62	4.20 – slope at V_{OC}
5	Arco 560 W array	3.05	-8.97	12.67 – slope at V_{OC}
6	Mobil 1800 W array	2.61	-0.56	2.63 – slope at V_{OC}
7	Trisolar 4500 W array	0.76	0.17	1.2 – slope at V_{OC}
8	Arco 43 W module	0.09	0.04	0.056 – given by mfg.
9	Applied Solar 71 W module	0.11	0.24	.21 – Method 4 (using data from system #8)

Method 3, using a maximum power point constraint, yields erratic and often impossible negative results. For some of the systems, the predicted value seems to have a reasonable magnitude but incorrect sign, and for others, the values seem consistent with the other methods. Two explanations for this behavior are:

1. As discussed in Sections 2.3.2 and 2.3.3, the forms of the L4P and other I-V equations are based on simplifying assumptions regarding the lumped vs. distributed nature of the circuit elements. These simplifications limit their ability to precisely model I-V behavior. Wolf [23] observed that models based on lumped equivalent circuits were less accurate near the maximum power point than at other positions on the I-V curve, when compared to actual curves. The simplified equations have too few parameters to be both exact enough and flexible enough to always force the measured maximum power

point to match the analytical maximum power point.

2. The equations are highly sensitive to small changes in input terms like I_{MP} and V_{MP}, Often, published values for these quantities are rounded off (up) to too few significant digits to satisfy four simultaneous equations.

It was asserted in an earlier paragraph that Method 5, the slope sampling method, overestimates the series resistance. This may be demonstrated analytically by starting with the root form of the L4P I-V equation, Equation 2.24. First, this equation is differentiated with respect to voltage and the resulting differential equation is evaluated at the open circuit voltage condition, where I = 0 and V = V_{OC}, Solving the equation for R_S gives:

$$R_S = \frac{-1}{\frac{\partial I}{\partial V}} - \frac{1}{\frac{qI_O}{\gamma kT_C}\exp\left(\frac{qV_{OC}}{\gamma kT_C}\right)} \qquad (2.38)$$

This equation shows that although the series resistance is related to the slope of the I-V curve at the open circuit condition, it is always smaller than the negative reciprocal of the I-V slope at the open circuit, by an amount equal to the second term on the right side of the equation. If the same equation is evaluated at higher voltages (i.e., as $I \rightarrow -\infty$), the second term becomes very small and the series resistance is then approximately equal to the slope of of the I-V curve at the higher voltage. This is demonstrated in Figure 15 for a large Tn-Solar Corp. array at the New Mexico Solar Energy Institute's (NMSEI) Southwest Regional Experiment Station. This corresponds to system 7 in Table 3. where the series resistance is estimated as 0.76 ohms by the iterative

method and 1.2 ohms by NMSEI. The curve shown was generated using the UP I-V model, and assumed a series resistance of 0.76 ohms. The slope of the generated curve at large negative currents corresponds *to* the correct value of R_S, while the slope at the open circuit point yields an R_S estimate equal to the NMSEI estimate, which is about 50% too high.

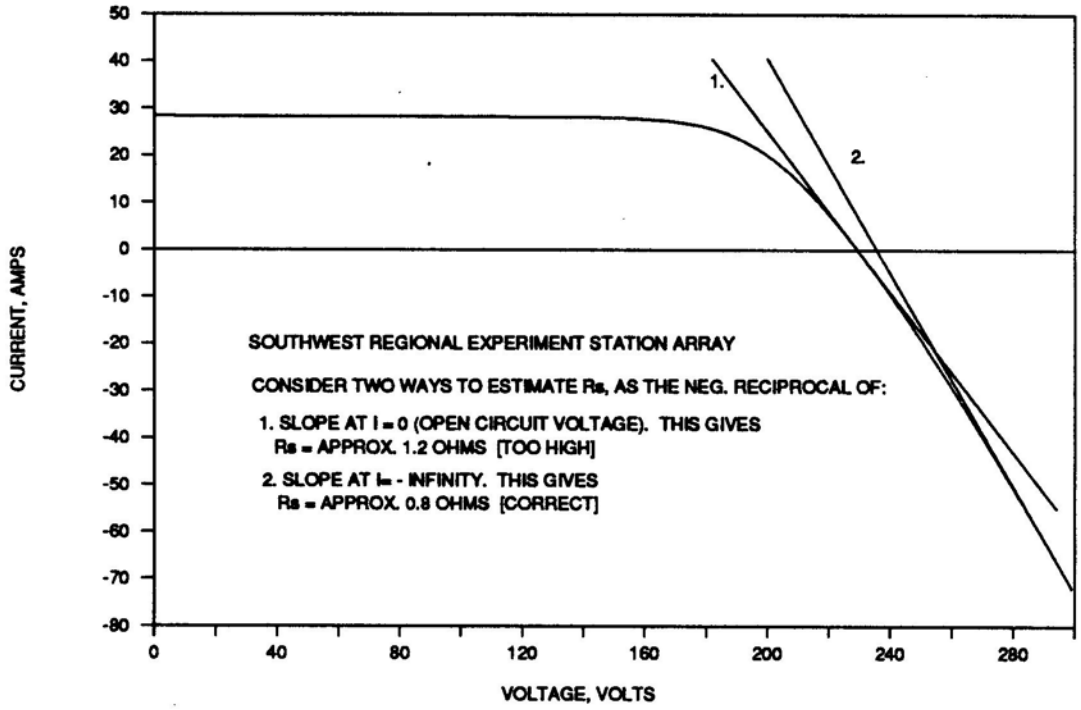

Figure 15. Graphical Interpretation of Series Resistance

Both Method 3, the maximum power point constraint method, and Method 2, the iterative method, are explained in detail in the following sections. The maximum power point method is developed first because the iterative method is derived from it. The solution procedure used in the long-term performance model uses the iterative method to

find R_S, but this may be overridden if a better estimate is available. Once the unknown parameters have been found, their values are inserted into the original I-V equation. The resulting I-V equation is a continuous analytical expression which gives I as an implicit function of V.

2.4.3 4 x 4 Solution Methods for the L4P I-V Model

The sequence of steps required to determine the unknown parameters for the L4P model begins with the basic I-V equation for the L4P circuit, Eqn 2.24. The four unknown parameters for this circuit are I_L, I_O, γ, and R_S. The other unknown variables in the original equation are I and V. Three new and independent versions of the equation are written by substituting measured values for I and V at three points on the curve. Any three points may be used. but the three commonly reported are:

- Short circuit current. where $I = I_{SC}$, $V = 0$
- Open circuit voltage, where $I = 0$, $V = V_{OC}$
- Maximum power point, where $I = I_{MP}$, $V = V_{MP}$

Each equation is set up as an objective function equal to zero, with all terms moved to one side of the equation.

$$F_1 = -I_{SC} + I_L - I_O\left(\exp\left(\frac{q}{\gamma kT_C}\times\left(I_{SC}R_S\right)\right)-1\right) \quad (2.39)$$

$$F_2 = 0 = I_L + I_O\left(\exp\left(\frac{q}{\gamma kT_C}\times\left(V_{OC}\right)\right)-1\right) \quad (2.40)$$

$$F_3 = 0 = -I_{MP} + I_L - I_O\left(\exp\left(\frac{q}{\gamma kT_C}\times\left(V_{MP}+I_{MP}R_S\right)\right)-1\right) \quad (2.41)$$

The next step is to derive a fourth independent objective function which forces the measured maximum power point to also be the maximum power point on the analytical curve. First, the power may be written as the product of I and V. and then Eqn. 2.24 is substituted for I:

$$P = I \times V \tag{2.42}$$

$$P = \left[I_L - I_O \left(\exp\left(\frac{q}{\gamma k T_C} \times \left(V + I R_S \right) \right) - 1 \right) \right] \times \left[V \right] \tag{2.43}$$

The power is then differentiated with respect to V and equated to zero:

$$\frac{dP}{dV} = 0 = \frac{\partial I}{\partial V} \times V + I \times \frac{\partial V}{\partial V} \tag{2.44}$$

The first term in Eqn. 2.44, the partial derivative of I with respect to V, is obtained by differentiating Eqn. 2.24:

$$\frac{\partial I}{\partial V} = -I_O \exp\left(\frac{q}{\gamma k T_C} \times \left(V + I R_S \right) \right) \times \frac{q}{\gamma k T_C} \times \left(1 + R_S \frac{\partial I}{\partial V} \right) \tag{2.45}$$

This is rearranged to solve for $\partial I/\partial V$ explicitly:

$$\frac{\partial I}{\partial V} = \frac{-I_O \frac{q}{\gamma k T_C} \exp\left(\frac{q}{\gamma k T_C} \times \left(V + I R_S \right) \right)}{\left(1 + R_S I_O \frac{q}{\gamma k T_C} \exp\left(\frac{q}{\gamma k T_C} \times \left(V \_ I R_S \right) \right) \right)} \tag{2.46}$$

Then substituting Eqn 2.46 into Eqn 2.44, rearranging, and inserting V_{MP} for V and I_{MP} for I yields a fourth independent equation (Figure 2 in Section 1.2 shows this to be a maximum):

$$F_4 = 0 = I_L + I_O - I_O \exp\left(\frac{q\left(V_{MP} + I_{MP} R_S \right)}{\gamma k T_C} \right) \times \tag{2.47}$$

$$\left(1 + \frac{\frac{qV_{MP}}{\gamma kT_C}}{\left(1 + R_S \frac{q}{\gamma kT_C} I_O \exp\left(\frac{q}{\gamma kT_C} \times \left(V_{MP} + I_{MP} R_S \right) \right) \right)} \right)$$

Functions F_1, F_2, F_3, and F_4 form a system of four non-linear equations in four unknown variables, x_1 thru x_4. In the derivations which follow, $I_L=x_1$, $I_O=x_2$, $\gamma=x_3$ and $R_S = x_4$. In the form shown, an iterative approach is required to solve the system of equations. Section 2.4.3.1 describes how to apply the Newton-Raphson method. However, an explicit solution via successive substitution is possible if the system of equations is simplified by omitting some minor terms. Section 2.4.3.2 details the simpler explicit method. Either method returns essentially the same values for the four unknown parameters. A sample comparison between the values returned by the two methods is shown in Section 2.4.3.3.

2.4.3.1 Newton-Raphson Method

Each objective function F_1 thru F_4 equals zero when the correct value for each of the four "x" variables is found. First, guesses are made for each variable. Then, a first order Taylor-series expansion is used to establish a new set of simultaneous equations in matrix form [34]. This requires computing the Jacobian matrix of the objective functions. Solving the new set of equations provides a better guess for each unknown, and the process is repeated until the difference between successive guesses lies within a desired tolerance. The form of the expansion for the first objective function is:

$$F_1\left(x_{1,T}, x_{2,T}, x_{3,T}, x_{4,T}\right) \approx F_1\left(x_{1,C}, x_{2,C}, x_{3,C}, x_{4,C}\right) +$$

$$\frac{\partial F_1\left(x_{1,T}, x_{2,T}, x_{3,T}, x_{4,T}\right)}{\partial x_2}\left(x_{2,T} - x_{2,C}\right) +$$

$$\frac{\partial F_1\left(x_{1,T}, x_{2,T}, x_{3,T}, x_{4,T}\right)}{\partial x_3}\left(x_{3,T} - x_{3,C}\right) +$$

$$\frac{\partial F_1\left(x_{1,T}, x_{2,T}, x_{3,T}, x_{4,T}\right)}{\partial x_4}\left(x_{4,T} - x_{4,C}\right) \qquad (2.48)$$

where subscripts T and C refer to temporary and correct values. The form is similar for the other three objective functions. The new set of equations in matrix form is:

$$\begin{bmatrix} \frac{\partial F_1}{\partial x_1} & \frac{\partial F_1}{\partial x_2} & \frac{\partial F_1}{\partial x_3} & \frac{\partial F_1}{\partial x_4} \\ \frac{\partial F_2}{\partial x_1} & \frac{\partial F_2}{\partial x_2} & \frac{\partial F_2}{\partial x_3} & \frac{\partial F_2}{\partial x_4} \\ \frac{\partial F_3}{\partial x_1} & \frac{\partial F_3}{\partial x_2} & \frac{\partial F_3}{\partial x_3} & \frac{\partial F_3}{\partial x_4} \\ \frac{\partial F_4}{\partial x_1} & \frac{\partial F_4}{\partial x_2} & \frac{\partial F_4}{\partial x_3} & \frac{\partial F_4}{\partial x_4} \end{bmatrix} \times \begin{bmatrix} x_{1,T} - x_{1,C} \\ x_{2,T} - x_{2,C} \\ x_{3,T} - x_{3,C} \\ x_{4,T} - x_{4,C} \end{bmatrix} = \begin{bmatrix} F_1 \\ F_2 \\ F_3 \\ F_4 \end{bmatrix} \qquad (2.49)$$

Solving this matrix usually requires the initial guesses to be within approximately an order of magnitude of the correct value. Otherwise, Newton's method may provide divergent and unstable iterative guesses. In practice, assuming an approximate value for the series resistance and then solving a simpler 3 x 3 system provides good initial guesses to use for the above 4 x 4 system. The Jacobian terms are:

$$\frac{\partial F_1}{\partial x_1} = 1.0 \qquad (2.50)$$

$$\frac{\partial F_1}{\partial x_2} = 1.0 - \exp\left(\frac{qI_{SC}R_S}{\gamma kT_C}\right) \qquad (2.51)$$

$$\frac{\partial F_1}{\partial x_3} = I_O \frac{qI_{SC}R_S}{\gamma^2 kT_C} \exp\left(\frac{qI_{SC}R_S}{\gamma kT_C}\right) \tag{2.52}$$

$$\frac{\partial F_1}{\partial x_4} = -I_O \frac{qI_{SC}}{\gamma kT_C} \exp\left(\frac{qI_{SC}R_S}{\gamma kT_C}\right) \tag{2.53}$$

$$\frac{\partial F_2}{\partial x_1} = 1.0 \tag{2.54}$$

$$\frac{\partial F_2}{\partial x_2} = 1.0 - \exp\left(\frac{qV_{OC}}{\gamma kT_C}\right) \tag{2.55}$$

$$\frac{\partial F_2}{\partial x_3} = I_O \frac{qV_{OC}}{\gamma^2 kT_C} \exp\left(\frac{qV_{OC}}{\gamma kT_C}\right) \tag{2.56}$$

$$\frac{\partial F_2}{\partial x_4} = 0.0 \tag{2.57}$$

$$\frac{\partial F_3}{\partial x_1} = 1.0 \tag{2.58}$$

$$\frac{\partial F_3}{\partial x_2} = 1.0 - \exp\left(\frac{q}{\gamma kT_C}\left(V_{MP} + I_{MP}R_S\right)\right) \tag{2.59}$$

$$\frac{\partial F_3}{\partial x_3} = I_O \frac{q}{\gamma^2 kT_C}\left(V_{MP} + I_{MP}R_S\right)\exp\left(\frac{q}{\gamma kT_C}\left(V_{MP} + I_{MP}R_S\right)\right) \tag{2.60}$$

$$\frac{\partial F_3}{\partial x_4} = -I_O \frac{q}{\gamma kT_C} I_{MP} \exp\left(\frac{q}{\gamma kT_C}\left(V_{MP} + I_{MP}R_S\right)\right) \tag{2.61}$$

$$\frac{\partial F_4}{\partial x_1} = 1.0 \tag{2.62}$$

$$\frac{\partial F_4}{\partial x_2} = 1.0 - \exp\left(\frac{q\left(V_{MP} + I_{MP}R_S\right)}{\gamma kT_C}\right)\times$$

$$\left(1.0+\frac{qV_{MP}}{\gamma kT_C\left(1+R_SZ\right)}-\frac{qR_SV_{MP}Z}{\gamma kT_C\left(1.0+R_SZ\right)^2}\right) \qquad (2.63)$$

where Z is:

$$Z=I_O\frac{q}{\gamma kT_C}\exp\left(\frac{q}{\gamma kT_C}\left(V_{MP}+I_{MP}R_S\right)\right) \qquad (2.64)$$

$$\frac{\partial F_4}{\partial x_3}=\frac{-Z\left(V_{MP}+I_{MP}R_S\right)}{\gamma}\left(1.0+\frac{qV_{MP}}{\gamma kT_C\left(1+R_SZ\right)}\right)-$$

$$ZV_{MP}\left[\frac{1}{\left(1+R_SZ\right)}-\frac{R_SI_Oq}{\gamma^2kT_C}\left(1+\frac{q\left(V_{MP}+I_{MP}R_S\right)}{\gamma kT_C}\right)\right] \qquad (2.65)$$

where Z is defined in Eqn. 2.64.

$$\frac{\partial F_4}{\partial x_4}=-ZI_{MP}\left[1+\frac{qV_{MP}}{\gamma kT_C\left(1+R_SZ\right)}\right]+\frac{Z^2V_{MP}\left[1+\frac{R_SqI_{MP}}{\gamma kT_C}\right]}{\left[1+R_SZ\right]^2} \qquad (2.66)$$

where Z is defined in Eqn. 2.64.

2.4.3.2 Simplified Explicit Method

The solution method outlined in the previous section, while rigorous, is fairly unstable when given poor initial guesses, and requires many computational steps to solve for the system parameters. As an alternative method, by omitting some smaller terms, the four objective functions (Eqns. 2.39. 2.40, 2.41, 2.47) can be simplified to the point where an explicit solution is possible via successive substitution.

On the right side of objective function F 2 (Eqn. 2.40), the quantity -1 is subtracted from an exponential quantity. The terms which make up the exponent of *e* are:

($q V_{OC}/\gamma k T_C$). Regardless of the size of the system, at the open circuit voltage point, the value of the exponent is about 12. Since *e* raised to the 12th power (1.6×10^5) is far greater than 1, omitting the -1 term does not significantly affect other quantities.

At the maximum power point (Eqn. 2.41), the exponential term is again much greater than 1 and the same simplification can be made. At the short circuit point (Eqn. 2.39) the voltage is zero and the exponential term is only about el, so upon first inspection, it would be inappropriate to drop the -1 term from objective function F_1.

The reason the -1 term exists in the first place is best understood by looking at a simple circuit (Figure 14, Eqn. 2.27) at its short circuit point. At zero voltage, no current flows through the diode. The "-1" must add to, and thereby cancel, the e^0 term so that the diode current is zero. It follows by inspection that the light current I_L is equivalent to the short circuit current I_{SC}.

For the L4P circuit at its short circuit point, I_L and I_{SC} are not equivalent. The series resistance causes a small potential difference across the diode in parallel with it, so a small portion of the light current (about one millionth) gets shunted through the diode instead of through the short circuited terminals. To several significant digits, though, the two terms are essentially the same. By assuming that the two terms are equal, solving for parameter I_L becomes trivial: $I_L = I_{SC}$, under all conditions.

By assuming that $I_L = IS_C$, everything else, including the "-1" term, is dropped

from Eqn. 2.39. In this case the -1 is not dropped because it is small relative to the exponential quantity added to it, but because the product of I_O and the entire term in parentheses is small enough (approx. 10^{-6} x I_L to neglect.

The simplified I-V equation describing the L4P circuit is:

$$I \approx I_L - I_O \exp\left(\frac{q}{\gamma k T_C} \times \left(V + IR_S\right)\right) \tag{2.67}$$

And the first three objective functions are written as:

$$F_1 = 0 \approx -I_{SC} + I_L \tag{2.68}$$

$$F_2 = 0 \approx I_L - I_O \exp\left(\frac{q}{\gamma k T_C} \times \left(V_{OC}\right)\right) \tag{2.69}$$

$$F_3 = 0 \approx -I_{MP} + I_L - I_O \exp\left(\frac{q}{\gamma k T_C} \times \left(V_{MP} + I_{MP} R_S\right)\right) \tag{2.70}$$

The fourth objective function may be obtained in the same manner as in Section 2.4.3, by differentiating the power with respect to voltage and equating to zero. It is easier, though, to first reduce the system of equations by making three substitutions. This simplifies the subsequent algebra.

- Replace each I_L with I_{SC}, using new objective function F1 (Eqn. 2.68)
- Let $\Lambda = q/(\gamma k T_C)$. This is simply a consolidation of the parameter γ and a group of constants that is repeated often. The solved value for γ will be found at the end of the calculations after solving for the temporary parameter Λ. (2.71)

- Using the new objective equation F_2 (Eqn. 2.69), first solve explicitly for I_O and then substitute for loin both I-V Eqn. 2.67 and objective function F_3, Eqn. 2.70.

With these substitutions, the I-V equation becomes:

$$I \approx I_{SC}\left[1-\exp\left(\Lambda\times\left(V-V_{OC}+IR_S\right)\right)\right] \tag{2.72}$$

And objective function F 3' the maximum power point equation, becomes:

$$F_3 = 0 \approx -I_{MP}+I_{SC}\left[1-\exp\left(\Lambda\times\left(V_{MP}-V_{OC}+I_{MP}R_S\right)\right)\right] \tag{2.73}$$

Objective functions F_1 and F_2 have already been used to eliminate two parameters, I_L and I_O. The next steps are to create a fourth objective function starting with Eqn. 2.72, and then use it and Eqn. 2.73 to solve for the remaining two parameters, R_S and Λ. Objective function F_4 is:

$$F_4 = \frac{dP}{dV} = 0 = \frac{\partial I}{\partial V}\times V + I + \frac{\partial V}{\partial V} \tag{2.74}$$

The first term in Eqn. 2.74, the partial derivative of I with respect to V, is obtained by differentiating Eqn. 2.72 and then rearranging terms to give:

$$\frac{\partial I}{\partial V} = \frac{-I_{SC}\Lambda\exp\left(\Lambda\left(V-V_{OC}+IR_S\right)\right)}{\left(1+R_S I_{SC}\Lambda\exp\left(\Lambda\left(V-V_{OC}+IR_S\right)\right)\right)} \tag{2.75}$$

Substituting Eqn 2.75 into Eqn 2.74, rearranging, and inserting $V = V_{MP}$ and $I = I_{MP}$ gives the fourth objective function:

$$F_4 = 0 = 1-\exp\left(\Lambda\left(V_{MP}-V_{OC}+I_{MP}R_S\right)\right)\times$$

$$\left(1+\frac{\Lambda V_{MP}}{\left(1+\Lambda R_S I_{SC}\Lambda\exp\left(\Lambda\left(V_{MP}-V_{OC}+I_{MP}R_S\right)\right)\right)}\right) \tag{2.76}$$

The next step is to rearrange Eqn. 2.73, solve explicitly for RS, and then substitute the resulting expression into F4. This leaves one equation in just one unknown, Λ. Canceling terms and solving for A yields (skipping several algebraic steps):

$$\Lambda = \frac{\left[\frac{I_{SC}}{I_{SC} - I_{MP}} + \ln\left(1 - \frac{I_{MP}}{I_{SC}}\right)\right]}{2V_{MP} - V_{OC}} \tag{2.77}$$

With A known, the other parameters can be found by reverse substitution using the following equations (one parameter, I_L, was found to have a trivial solution, $I_L = I_{SC}$):

$$R_S = \frac{\frac{1}{\Lambda}\ln\left(1 - \frac{I_{MP}}{I_{SC}}\right) + V_{OC} - V_{MP}}{I_{MP}} \tag{2.78}$$

$$I_O = I_{SC}\exp\left(-\Lambda V_{OC}\right) \tag{2.79}$$

$$\gamma = \frac{q}{\Lambda k T_C} \tag{2.80}$$

Each of the four solved parameters is then used in the I-V equation (2.67) to get a continuous (implicit) expression relating I and V at a single condition of irradiance and cell temperature.

2.4.3.3 Sample Comparison: Newton and Simplified Methods

To compare the solved values of each parameter by both the Newton-Raphson method and the simplified explicit method a common set of inputs is used. The module selected for the comparison is an ARCO M-52, nominally rated at 43 Watts at 1000 W/m2 and a cell temperature of 25 C. Table 4 lists the inputs needed for the comparison.

Table *5* compares the results. The values are virtually equal for each parameter. For this reason, the simplified explicit method is preferred over the Newton-Raphson med1od.

Table 4. Sample Inputs for Comparing Two I. V Curve Solution Methods

Module:	ARCO M-52, 43 Watt nameplate
Irradiance:	1033.9 W/m^2
Cell Temperature:	33.35°C (306.5K)
Short Circuit Current, I_{SC}:	7.811 A
Open Circuit Voltage, V_{OC}:	6.808 V
Max. Pwr. Point Current, I_{MP}:	7.183 A
Max. Pwr. Point Voltage, V_{OC}:	5.389 V

Table 5. Solved Parameter Values Via Two I-V Curve Solution Methods

Parameter	Value using Newton-Raphs on Method	Value using Simplified Explicit Method	% difference
I_L	7.811 A	7.811 A	0.0
I_O	1.7851E-06 A	1.7849E-06 A	-0.01
γ	16.8563	16.8562	-0.0006
R_S	0.0413106 Ω	0.0413112 Ω	0.001

2.4.4 3 x 3 Solution Method for the L4P I-V Model

As stated in Section 2.4.2, attempting a simultaneous solution in four unknown parameters sometimes yields unrealistic results. This occurs whether the Newton-Raphson (Section 2.4.3.1) or explicit (Section 2.4.3.2) solution method is used. In this section, an alternate solution method is described. This method is useful if the series resistance parameter is known (or approximately known), which reduces the number of unknowns to three. The remaining three parameters are found using a simple explicit equation. In the next section, a procedure is developed which iterates with improved

guesses for R_S until a proper solution is obtained.

The solution method which follows is simpler than that used when the series resistance is unknown, because the added algebra associated with a fourth objective equation is omitted.

The solution begins with the maximum power relation given in Eqn. 2.73 from Section 2.4.3.2. This equation has already been reduced to a form where two of the three remaining unknown parameters have been eliminated. This reduction was accomplished by substituting Eqns. 2.68 and 2.69 into Eqn. 2.70, and by replacing $q/(\gamma\ k\ T_C)$ with Λ, according to Eqn. 2.71. Rearranging to solve for Λ gives:

$$\Lambda = \frac{\ln\left(1 - \frac{I_{MP}}{I_{SC}}\right)}{\left(V_{MP} - V_{OC} + IR_S\right)} \tag{2.81}$$

As with the earlier explicit solution method, the remaining parameters ~, 10, and γ are determined by reverse substitution using Eqns. 2.68 (trivial solution), 2.79, and 2.80.

Each parameter is used in the final I-V equation (2.67) to get a continuous expression which gives I implicitly as a function of V. at a single condition of irradiance and cell temperature.

2.4.5 Iterative Method to match μ_{VOC}

The temperature coefficient of open circuit voltage, μ_{VOC}, is an additional piece of

information ordinarily reported by PV manufacturers which can be used to help estimate the series resistance. This coefficient is measured at the reference irradiance and is assumed constant. If the proper value of series resistance is chosen, and the remaining parameters are calculated using equations from the preceding section, the proper value of μ_{VOC} may be derived analytically from the solved UP I-V model. In such a case, the reported value of μ_{VOC} is redundant. In this section, a procedure is developed where:

- Lower and upper limits for the series resistance are calculated.
- An analytical estimate of μ_{VOC} is compared to the reported value for the upper and lower limits for R_S.
- A binomial search routine is used to converge on the proper value of μ_{VOC} by making new guesses for R_S.

The lower limit for R_S must be zero ohms. The corresponding value for A is calculated using Eqn. 2.78 with $R_S = 0$, and then I_O is found using Eqn. 2.79. γ is calculated using Eqn. 2.80, and the last parameter, I_L, is set equal to I_{SC}. With the calculated parameter values inserted, I-V Eqn. 2.67 is capable of describing a complete I-V curve.

An upper limit for R_S can be derived based on a practical physical limit imposed by another cell parameter, γ. When a value for R_S is arbitrarily selected, the remaining parameters are fixed, according to the relationships developed in the previous section. The resulting I-V equation describes a line which must pass through the short circuit, open circuit, and maximum power points. A limited range of series resistances may be

selected which will describe differently shaped I-V curves, but each obeys the same three point constraint. Progressively higher values of R_S result in progressively lower values of γ. γ is the product of the completion factor, A, and the number of cells in series within the system, NCS. The completion factor has a lower limit of 1.0, which corresponds to a condition in which each photon-generated charge pair contributes perfectly to the cell current rather than recombining. Therefore, γ has a lower limit equal to the number of cells in series, a known quantity for each system.

Substituting γ = NCS into Eqn. 2.80 and then inserting the resultant value for A into Eqn. 2.78 yields the following upper limit for $R_S = R_{S,MAX}$:

$$R_{S,MAX} = \frac{1}{I_{MP}}\left[\frac{(NCS)kT_C}{q}\ln\left(1-\frac{I_{MP}}{I_{SC}}\right)+V_{OC}-V_{MP}\right] \quad (2.82)$$

I_L which is set equal to I_{SC}, is not affected by the value of γ. but I_O is. I_O is recalculated according to Eqn. 2.79, and then each calculated parameter is used in I-V Eqn. 2.67, as with the zero resistance case.

At the open circuit voltage point, Eqn. 2.67 may be rewritten to solve explicitly V_{OC}:

$$V_{OC} = \frac{\gamma kT_C}{q}\ln\left(\frac{I_{SC}}{I_O}\right) \quad (2.83)$$

Differentiating this expression with respect to cell temperature, at constant

irradiance, results in the following expression, which is set equal to the manufacturers' stated value for μ_{VOC}:

$$\mu_{VOC} = \frac{\partial V_{OC}}{\partial T_C} = \frac{\gamma k}{q}\left[\ln\left(\frac{I_{SC}}{I_O}\right) + \frac{T_C \mu_{ISC}}{I_{SC}} - \left(3 + \frac{q\varepsilon_G}{AkT_C}\right)\right] \quad (2.84)$$

At the proper value of R_S. the empirical and analytical quantities are equal. A binomial search routine was used in the long-term performance model to converge on the proper value for R, between the established upper and lower bounds. The final value for R_S fixes the value of the other parameters in I-V Eqn. 2.67 at the reference conditions.

The results of this solution method for nine systems were shown earlier in Table 3 of Section 2.4.2. This solution method seems more consistent than the maximum power point constraint method, and this is likely due to the fact that the L4P I-V equation is a better predictor of I-V behavior near the open circuit point than at the maximum power point. Like the maximum power point method. this method is also sensitive to the precision of the input data; therefore, round off error may lead to inaccurate solutions.

2.4.6 Information required to use the L4P I-V Model

Table 6 is a complete list of the information needed to use the UP I-V curve model for all irradiance levels and temperatures. Each item is ordinarily obtained from a PV manufacturer's module brochure, except for the apparent series resistance, which is often missing, and the semiconductor bandgap energy, which is published in many texts. The last three items are used to calculate cell temperature from a known ambient

temperature and irradiance. The procedure for doing so is explained in detail in Section 2.6.

Table 6. Information required to use the L4P I. V Model

Symbol	Units	Name	From mfg?
Φ_{REF}	W/m^2	plane of array irradiance, reference	Yes
Φ	W/m^2	plane of array irradiance	No
$T_{C,REF}$	K	cell temperature, reference	Yes
T_C	K	cell temperature	No
$I_{SC,REF}$	A	short circuit current, reference	Yes
$V_{OC,REF}$	V	open circuit voltage. reference	Yes
$I_{MP,REF}$	A	maximum power point current reference	Yes
$V_{MP,REF}$	V	maximum power point voltage, reference	Yes
NCS	1/system	number of cells in series within the system	Yes
μ_{ISC}	A/K	temperature coefficient of shan circuit current	Yes
μ_{VOC}	V/K	temperature coefficient of open circuit voltage	Yes
ε_G	V	bandgap energy - semiconductor material property, assumed constant over flat plate PV operating temperatures; published in many texts	No
R_S	Ω	apparent (lumped) series resistance - if not pro- vided by manufacturer, can be estimated by other methods (Section 2.4.2)	Some
Area	m^2	net module area	Yes
$T_{A,NOCT}$	K	ambient temperature at Nominal Operating Cell Temperature (NOCT) test conditions	Yes
Φ_{NOCT}	W/m^2	plane of array irradiance at NOCT conditions	Yes
$T_{C,NOCT}$	K	cell temperature at NOCT conditions	Yes

2.5 Effects of Irradiance and Temperature on I-V Characteristics

Much of the computational effort needed to describe I-V behavior is associated with initially solving for the unknown parameters at a reference irradiance and cell temperature. Although a new I-V curve is needed when either the irradiance or temperature changes, fewer computations are needed to update parameter values once the reference values are established. This is because auxiliary relationships are used to track the changes in parameters from their reference values, rather than solve an entire system of equations at each new set of conditions. Solving a new system of equations at each new set of conditions is ordinarily not possible, because the three I-V curve points (inputs I_{SC}, V_{OC}, and I_{MP}-V_{MP}) are only known at one condition.

Of the four parameters in the L4P model, I_L is assumed to vary with irradiance and temperature according to Eqn. 2.2. I_O is assumed to vary only with temperature according to Eqn. 2.4, and R_S and γ are assumed constant, at least over the expected range of temperatures and irradiances for flat plate PV modules. Figure 16 illustrates the dependence of I-V characteristics on temperature and irradiance for a sample module. The trends evident in this plot are similar for other PVs, namely, the strong effect of irradiance on short circuit current and of temperature on open circuit voltage, and the weaker effect of irradiance on open circuit voltage and of temperature on short circuit current.

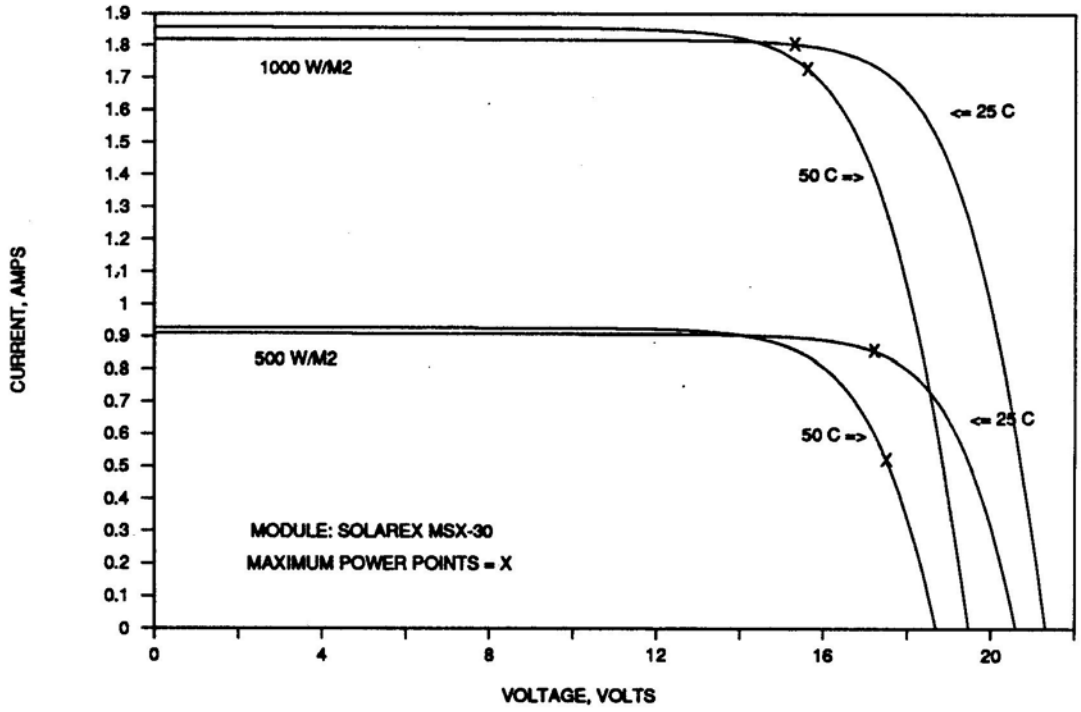

Figure 16. Effect of Irradiance, Temperature on I-V Curve Shape

2.6 Determining Cell Temperature

The temperature within an illuminated PV cell is related to the ambient temperature, and also to the rates at which incident energy is being absorbed, dissipated, and converted to electricity. A steady state energy balance determines the average cell temperature increase above ambient. Because the cells are thin and have a small heat capacity, temperature gradients across the cell are neglected in the following analysis. Under normal operating conditions (i.e., no shaded or failed cells), the average temperature of each cell within a module or an array is approximately the same.

D.C. POWER = ABSORBED POWER – DISSIPATED POWER (2.85)

where each te1'ID may be funher broken down as:

$$\text{D.C. POWER} = \Phi \times Area \times \eta \tag{2.86}$$

η is the dimensionless D.C. electric conversion efficiency. It ranges from zero at the short circuit and open circuit points to a typical maximum of about 10 -14% at the maximum power point.

$$\text{ABSORBED POWER} = \Phi \times Area \times \left(\overline{\tau\alpha}\right) \tag{2.87}$$

$\left(\overline{\tau\alpha}\right)$ is the dimensionless transmittance-absorptance product, or the ratio of absorbed to incident energy

$$\text{DISSIPATED POWER} = U_L \times Area \times \left(T_C - T_{AMB}\right) \tag{2.88}$$

U_L is an overall (convective and radiative) loss coefficient, with units of $W/m^2 \bullet K$. For simplicity, the loss coefficient is assumed to be constant, which neglects the effect that factors such as windspeed, humidity, and temperature may have on it. Although these factors may substantially affect the loss coefficient, their effect on the resulting absolute (Kelvin) cell temperature is small.

Substituting Eqns. 2.86 - 2.88 into 2.85 and then rearranging to solve for T_C gives:

$$T_C = T_{AMB} + \frac{\Phi\left(\overline{\tau\alpha}\right)}{U_L}\left(1 - \frac{\eta}{\left(\overline{\tau\alpha}\right)}\right) \tag{2.89}$$

The transmittance-absorptance product is assumed constant at 0.9, with no correction for dependence on incidence angle. Another simplifying assumption is to assign a constant value for 11- Even though 11 varies from 0 to about 14%, depending on the applied load and the weather conditions, selecting a constant value does not

significantly affect the cell temperature calculation. This is due to the fact that, of the terms in parentheses, $\eta/(\overline{\tau\alpha}) << 1$. At a typical average irradiance of about 600 W/m^2, the difference in calculated cell temperature between 5% and 14% efficiency (starting at 0%, the comparison is meaningless, since the power output is zero) is less than 2 °C. This is about the same uncertainty inherent in cell temperature measurements, and amounts to less than a 1 % difference in power output near the maximum power point.

The value of η chosen for Eqn. 2.89 is the maximum power point efficiency at the given reference conditions. η_{REF}. and is calculated from:

$$\eta_{REF} = \frac{I_{MP,REF} V_{MP,REF}}{\Phi_{REF} Area} \tag{2.90}$$

To find the loss coefficient U_L, three pieces of information from a standard test procedure called the Nominal Operating Cell Temperature (NOCT) test are needed. This information is given by the module manufacturer, and is listed in Table 6. The NOCT test measures the steady state cell temperature when the system is open-circuited (efficiency = 0.0) at a standard set of conditions; usually, at an ambient temperature of 20°C, a plane of array irradiance of either 800 or 1000 W/m^2, and a wind speed of 1 m/s, not predominantly parallel to the array. The resulting cell temperature is ordinarily 40 - 50°C. At the NOCT test conditions. Eqn. 2.89 is rewritten to solve for U_L:

$$U_L = \frac{\Phi_{NOCT}(\overline{\tau\alpha})}{T_{C,NOCT} - T_{AMB,NOCT}} \tag{2.91}$$

U_L is substituted back into Eqn. 2.89 and used for each hourly calculation of cell temperature.

2.7 Effect of Series/Parallel Groupings on I-V Characteristics

Sections 2.4.3 thru 2.4.5 detailed methods by which the various unknown parameters may be determined for the UP I-V model. The input data is ordinarily based on a single module's measured I-V characteristics at some reference condition. For an array of two or more modules, the parameters need to be scaled up to describe array-level I-V characteristics. The scaling depends on the number of series (NS) and parallel (NP) strings of modules making up the array. The scaling relationships for the L4P I-V model parameters are:

Array Value = Module Value x Scaling Term	
Parameter	Scaling Term
I_L	NP
I_O	NP
γ	NS
R_S	NS/NP

These relationships assume that all modules in the array are alike. For a real array, the overall value of any of the four parameters will differ from the scaled values because all modules are not identical. This type of mismatch penalizes output and cannot be eliminated. but can be minimized by testing each module's output under uniform conditions prior to array assembly and then accepting only those modules whose output falls within normal tolerances. Typical array mismatch losses may range from 1-5% [12,35]. For production tolerances of ± 5-10%, mismatch losses are not significant [36].

Throughout this study, each module within an array is assumed to be identical. This assumption yields upper performance limits of the array.

Figure 17 shows how the I-V curve shape for a single module changes when additional modules are wired in series and parallel groupings.

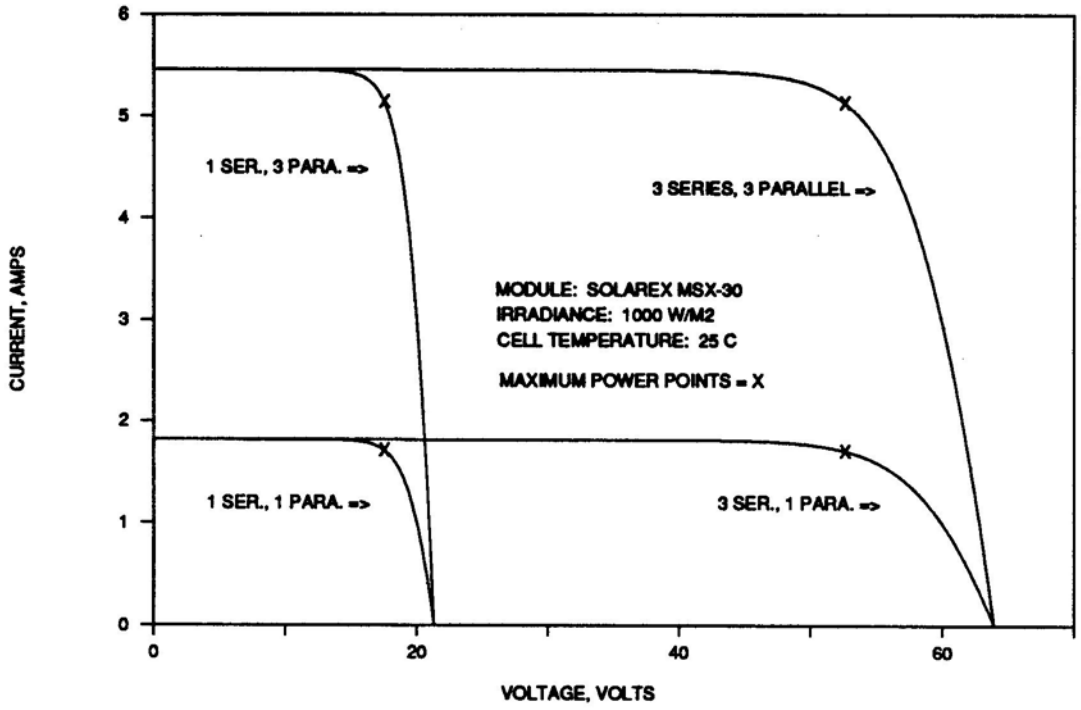

Figure 17. Effect of Series/Parallel Arrangement on I -V Curve Shape

2.8 I-V Models Compared to Measured Data

The five I-V curve models outlined in Section 2.3.3 differ in their ability to predict the I-V curve characteristics of actual PV systems. In this section, the I-V models are evaluated two ways. The first is a comparison of I-V and Power- V curves generated

by each model, relative to measured I-V points at the same irradiance and cell temperature. Curves for two module types are examined. The second way is a statistical comparison of the predicted maximum power point output for three systems, relative to data measured under a range of operating conditions.

2.8.1 I- V Curves

To allow a consistent set of comparisons for a given module, the same reference condition is selected for each I-V model. For the three I-V models which include series resistance as a fourth unknown parameter (L4P, MIT, 2M6P), the same value of R_S, is used in each.

At the reference condition, differences between the I-V models are minor. This is because each is forced to trace a smooth curve through the same three points (short circuit, open circuit. and maximum power points). Differences between models become more apparent under conditions farther away from the reference condition. The following plots use variations in irradiance and temperature to illustrate differences between models.

Figures 18a, 18b, and 18c are I-V plots for an Applied Solar Corp. module with a nominal peak rating of 75 W at about 16 volts. Each of the five I-V models are compared to actual points measured by the Pacific Gas and Electric Co. [30]. The irradiance (1030 W/m^2) and cell temperature (36 °C) shown are also selected to be the reference condition. For clarity, three plots are presented, because some of the I-V curves would otherwise be

indistinguishable. The UP (on both Figs. 18a,c) and 2M6P (Fig. 18b) models are nearly identical and match well with the measured points. Both of these models, as well as the MIT model, assume R, = 0.21 ohms. At the reference condition, however, the series resistance term does not affect the MIT model (as explained in Section 2.3.3.5). The MIT, L3P. and 2M5P (R. = 0) curves are similar and do not follow the measured points as closely.

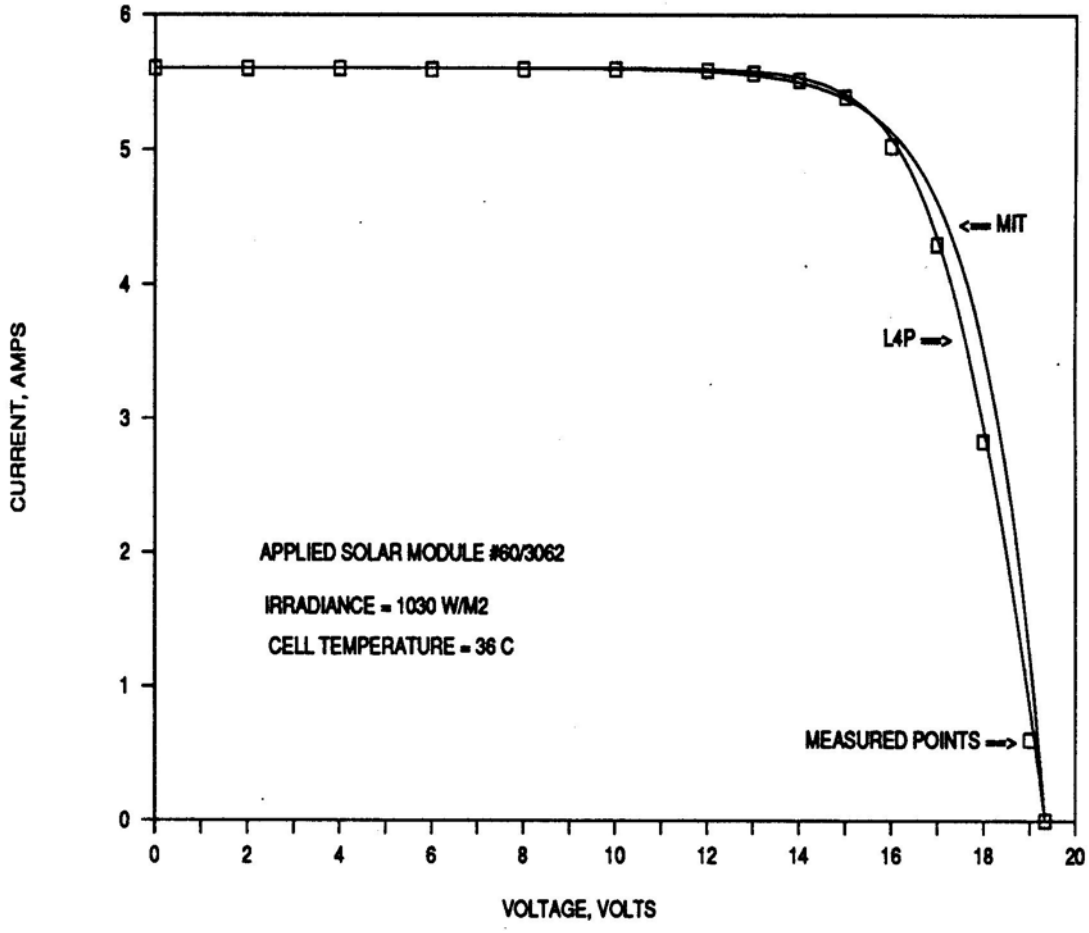

Figure 18a. I-V Curve Comparison for lAP and MlT Models

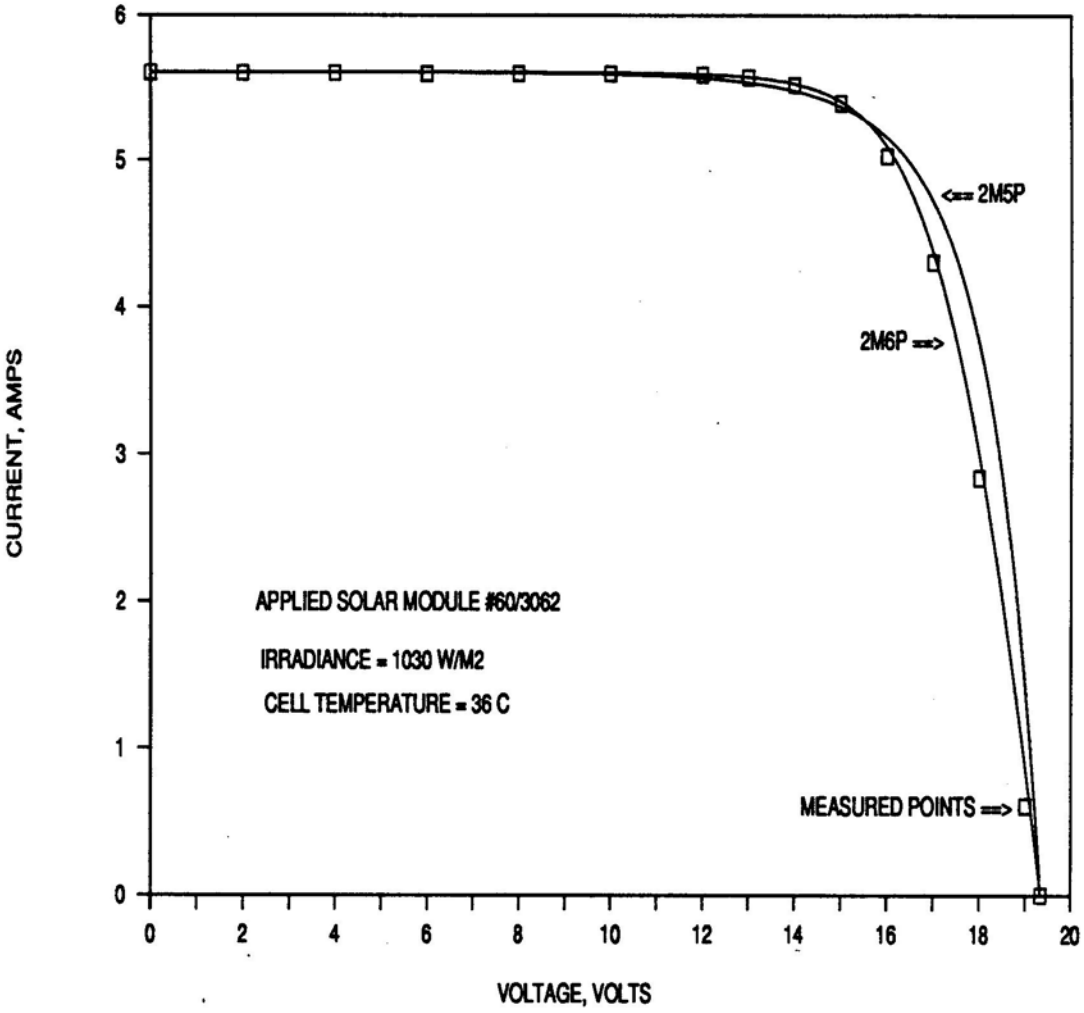

Figure 18b. I-V Curve Comparison for 2M5P and 2M6P Models

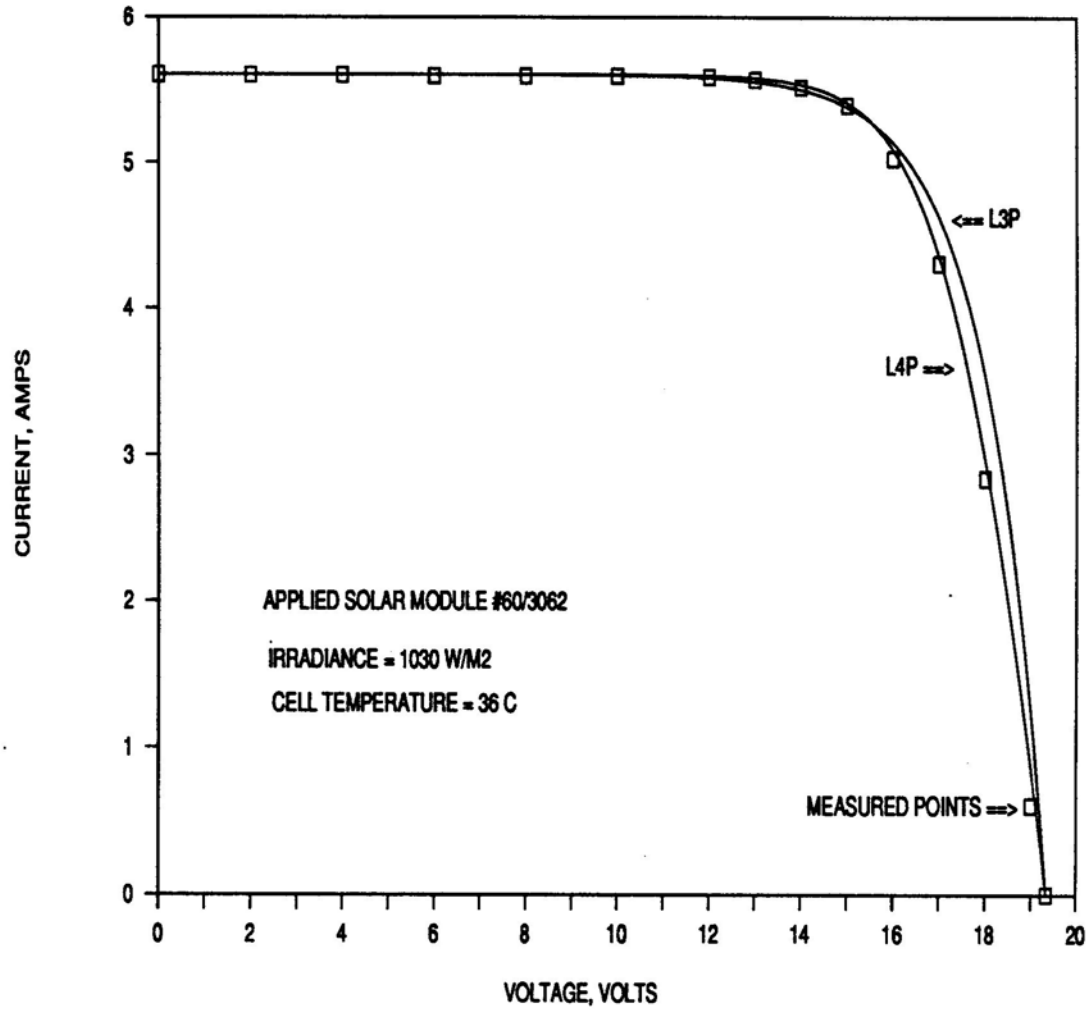

Figure 18c. I-V Curve Comparison for L3P and UP Models

To show how differences in I-V curve shape affect the predicted power output, the information from an I-V curve can be plotted instead on a power vs. voltage scale. Figure 19 is a rescaled Power-V plot of Figure 18a. Power-V plots for the other I-V models are not shown, but are similar. Table 7 lists the root mean square (RMS) % difference, averaged over the full Power- V curve, between the power (I x V) at 15

measured points versus that predicted by each model. The RMS % difference is calculated as:

$$RMS\%DIFF. = \left[\frac{\sum \left(P_{PRED.} - P_{MEAS.} \right)^2}{\#\, pts.} \right]^{1/2} \times \frac{100}{P_{MEAS.,AVG.}} \qquad (2.92)$$

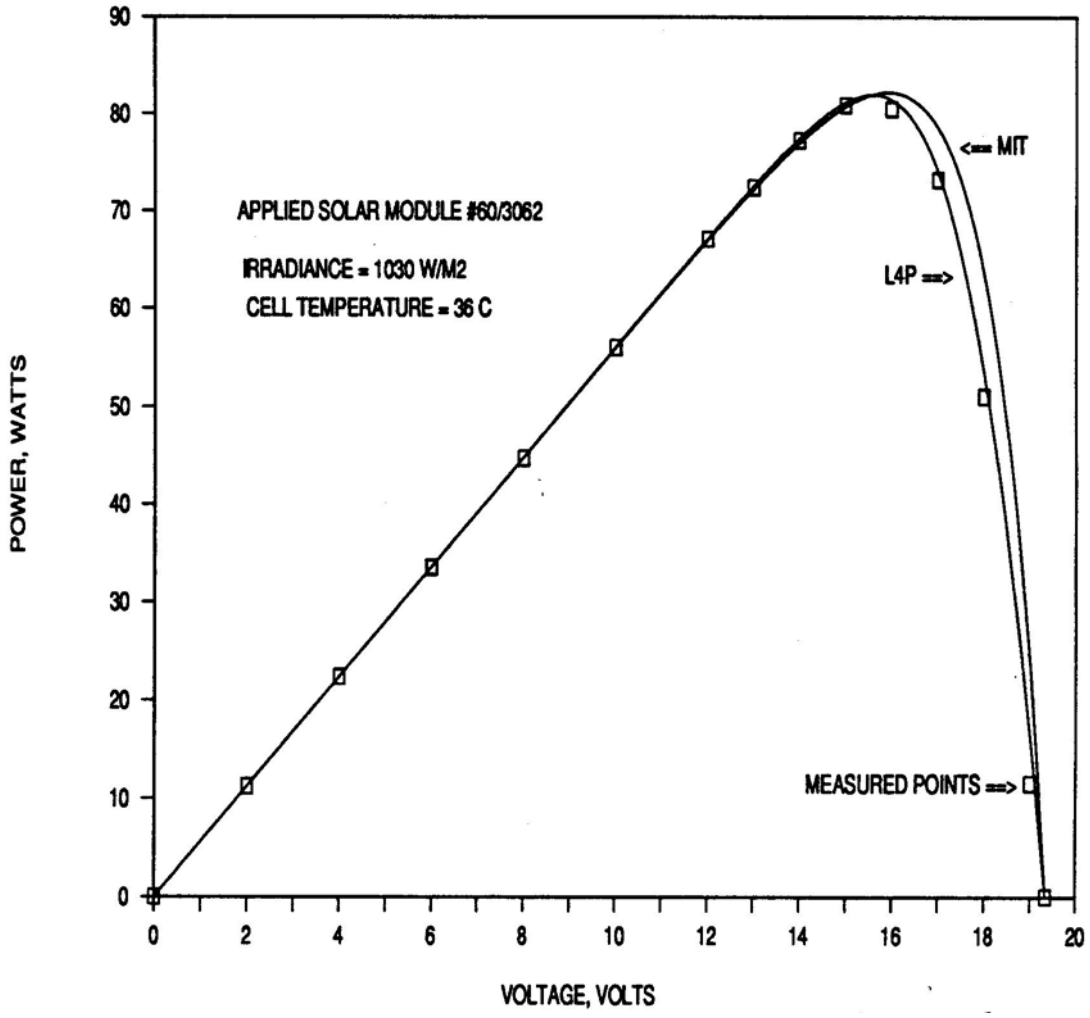

Figure 19. Power- V Curve Comparison for UP and MIT Models

Table 7. RMS % Power Differences, Applied Solar module

Irrad. = 1030 W/m^2, Cell Temp. = 36°C	
I-V Model	RMS % Power Difference over full Power- V curve
L3P	0.7
L4P	0.2
2M5P	0.9
2M6P	0.2
MIT	0.7

The effect of irradiance on predicted I-V curves is shown in Figures 20a and 20b. The reference irradiance and cell temperature are the same as in the previous figures, but the test irradiance is reduced to 338 W/m^2, about 1/3 that of the previous curves. Measured values for the short circuit, open circuit, and maximum power points are shown. At the lower irradiance, differences between the models are more apparent. Models which account for series resistance translate more accurately to the lower irradiance condition than those which do not account for series resistance.

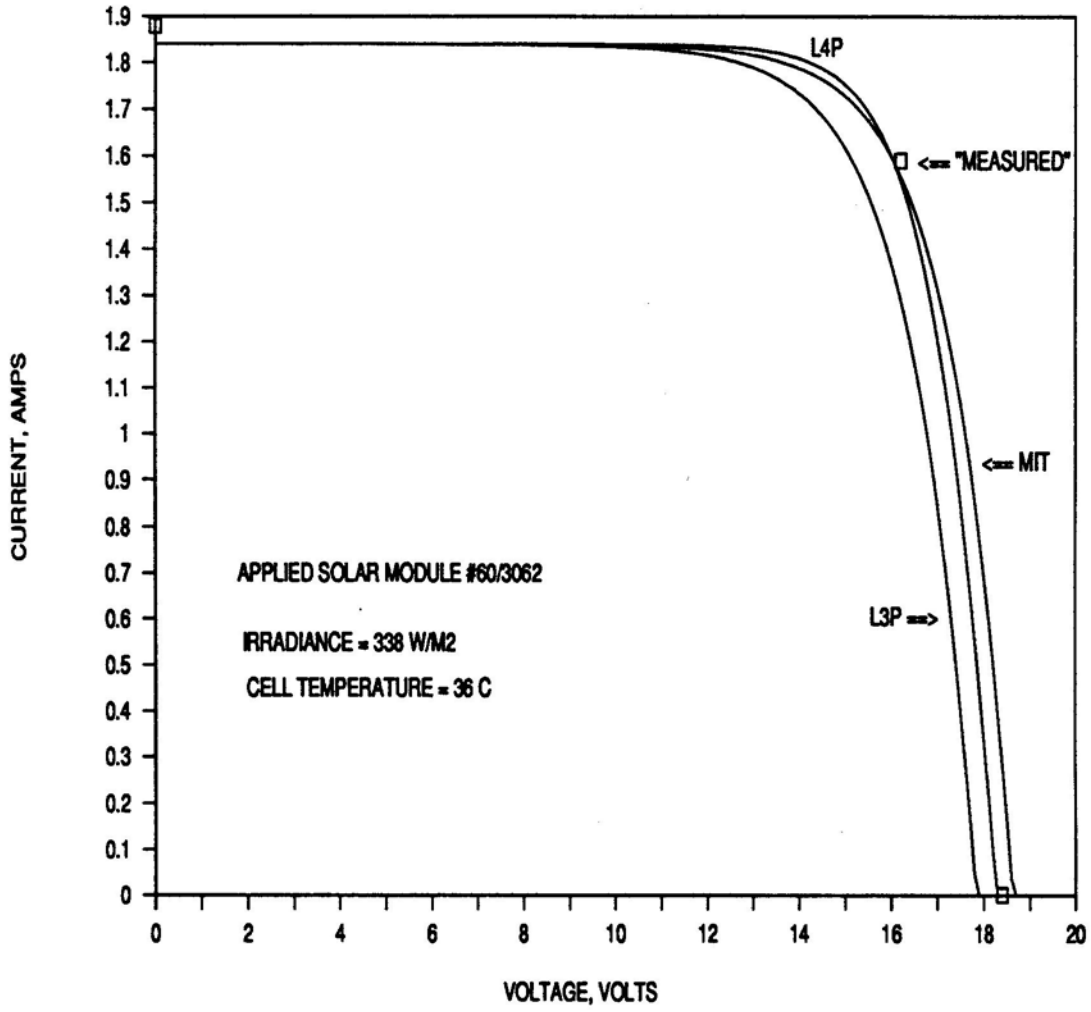

Figure 20a. I-V Curves for L3P, L4P, and MIT Models at Low Irradiance; Applied Solar module

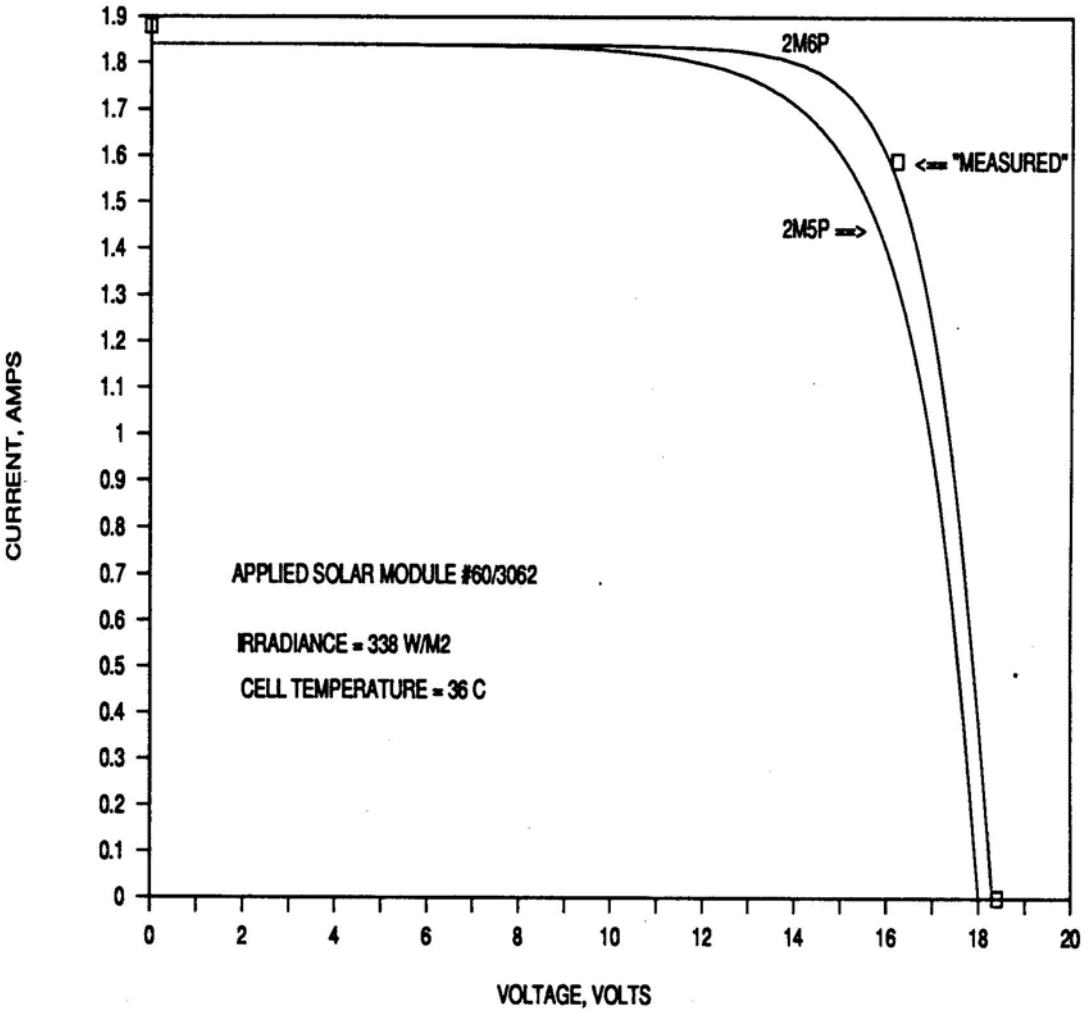

Figure 20b. I-V Curves for 2M5P and 2M6P Models at Low Irradiance; Applied Solar module

Figures 21a and 21b show the Power-V characteristics for the five models at the lower irradiance. The difference between the measured maximum power and predicted maximum power is about 1 % for the MIT model, 2% for the UP and 2M6P models, and 5% for the L3P and 2M5P models.

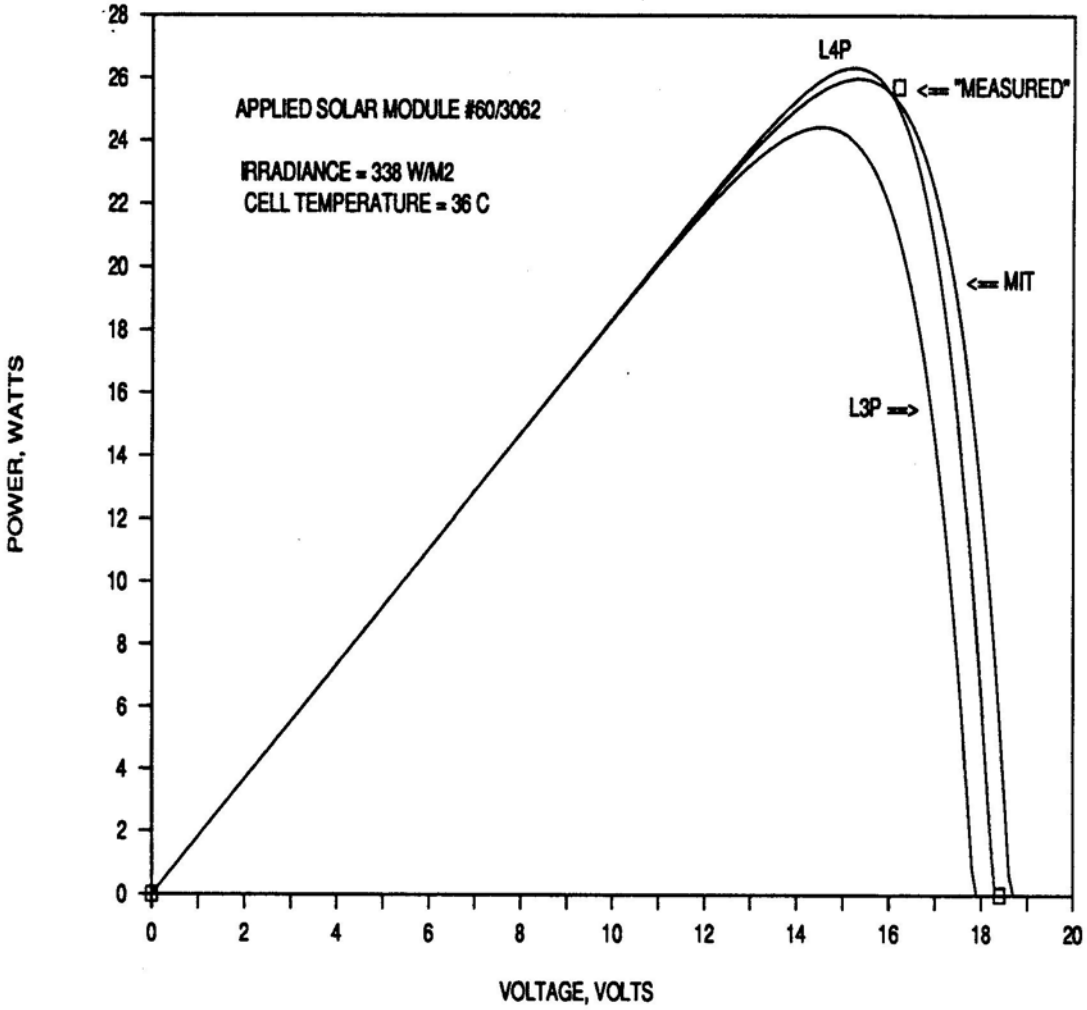

Figure 21a. Power- V Curves for the L3P, L4P, and MIT Models at Low Irradiance

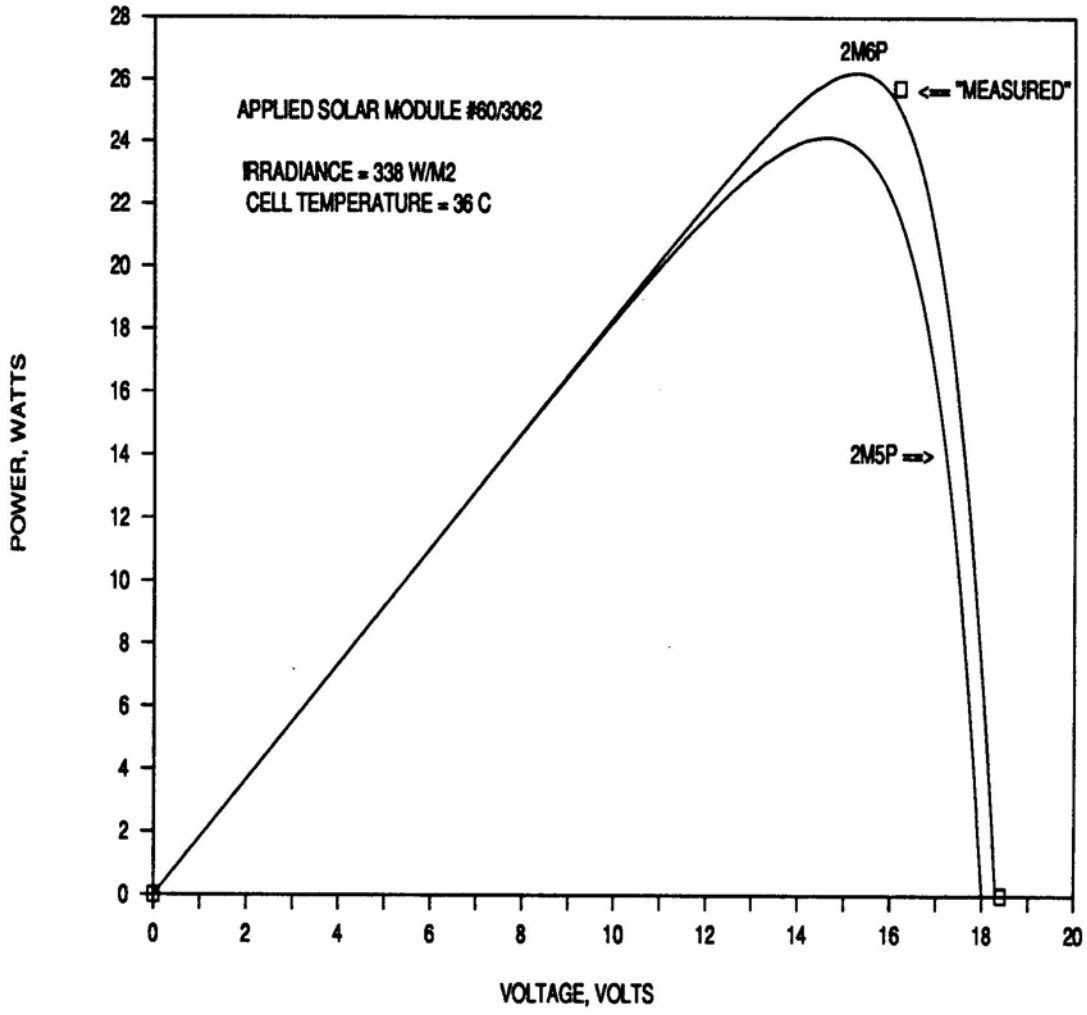

Figure 21b. Power-V Curves for 2M5P and 2M6P Models at Low Irradiance

The effect of changing irradiance on the various I-V models is also shown for another PGandE test module, an ARCO M-52, nominally rated at 43 W and 6 volts. For this module, the reference irradiance is 1034 W/m^2 and the reference cell temperature is 34 °C. Figures 22a and 22b compare the five I-V models to measured points at a test condition of 1027 W/m^2 and 43 °C. Figures 23a and 23b show the same results plotted on a Power- V scale. Table 8 lists the RMS % difference, over the full Power- V curve,

between the power (I x V) at 19 measured points versus that predicted by each model.

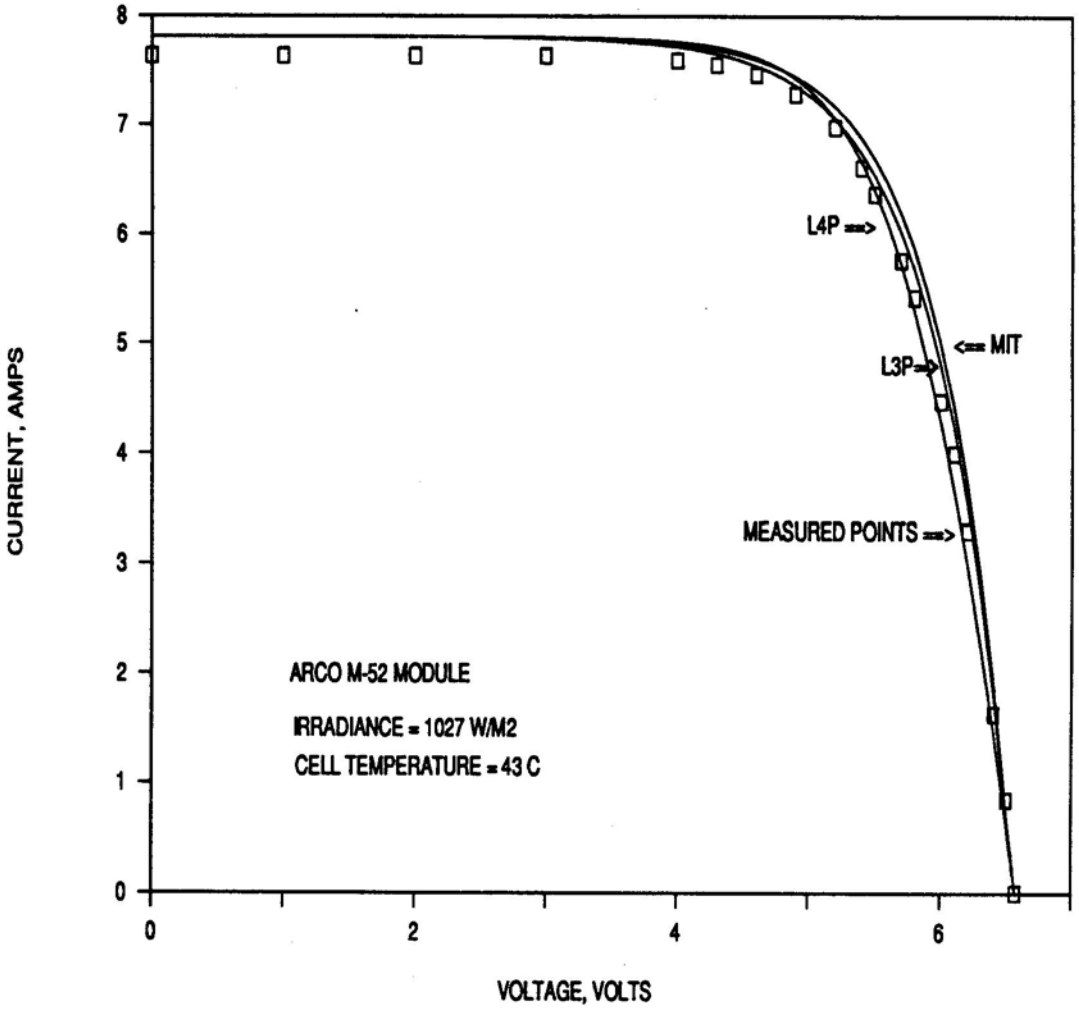

Figure 22a. ARCO I-V Curves compared for L3P, UP, and MIT Models

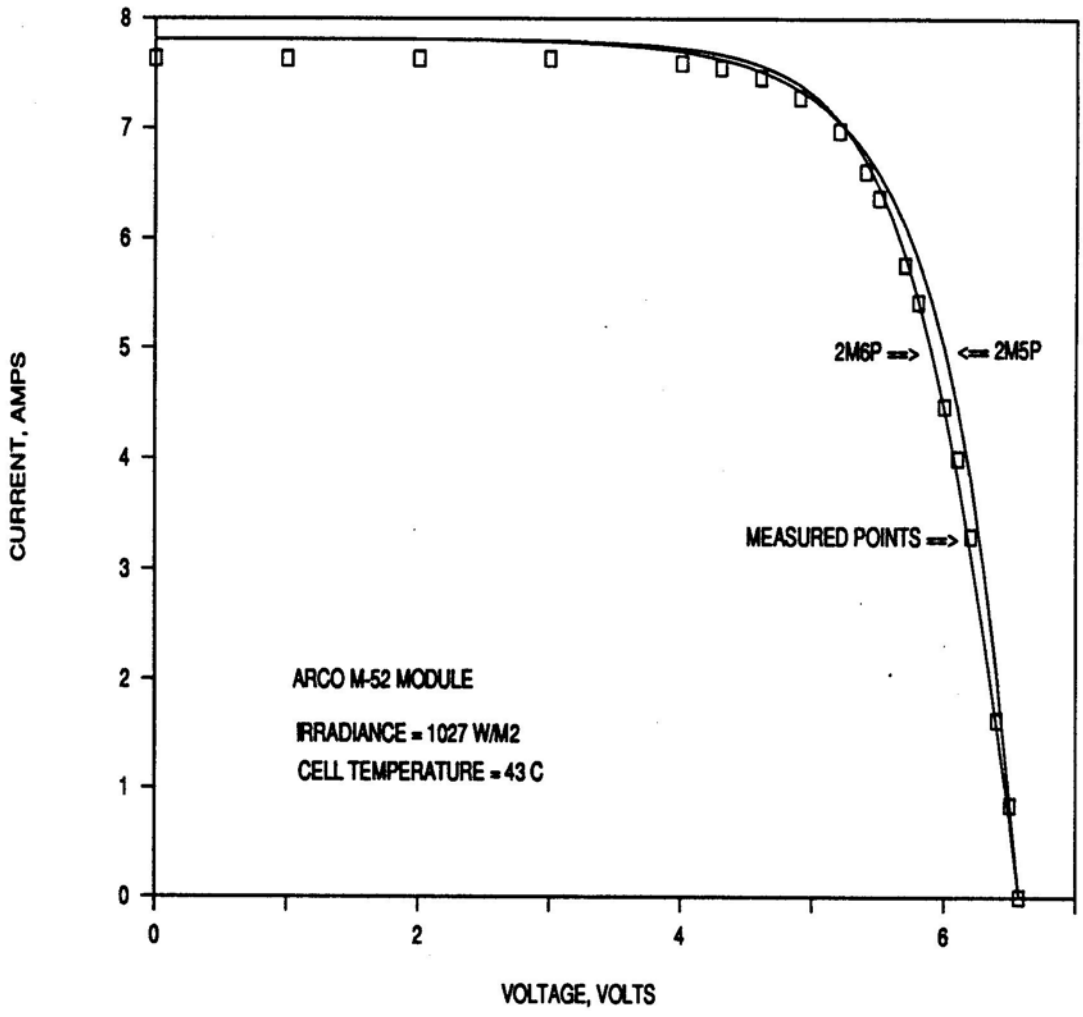

Figure 22b. ARCO I-V Curves compared for 2M5P and 2M6P Models

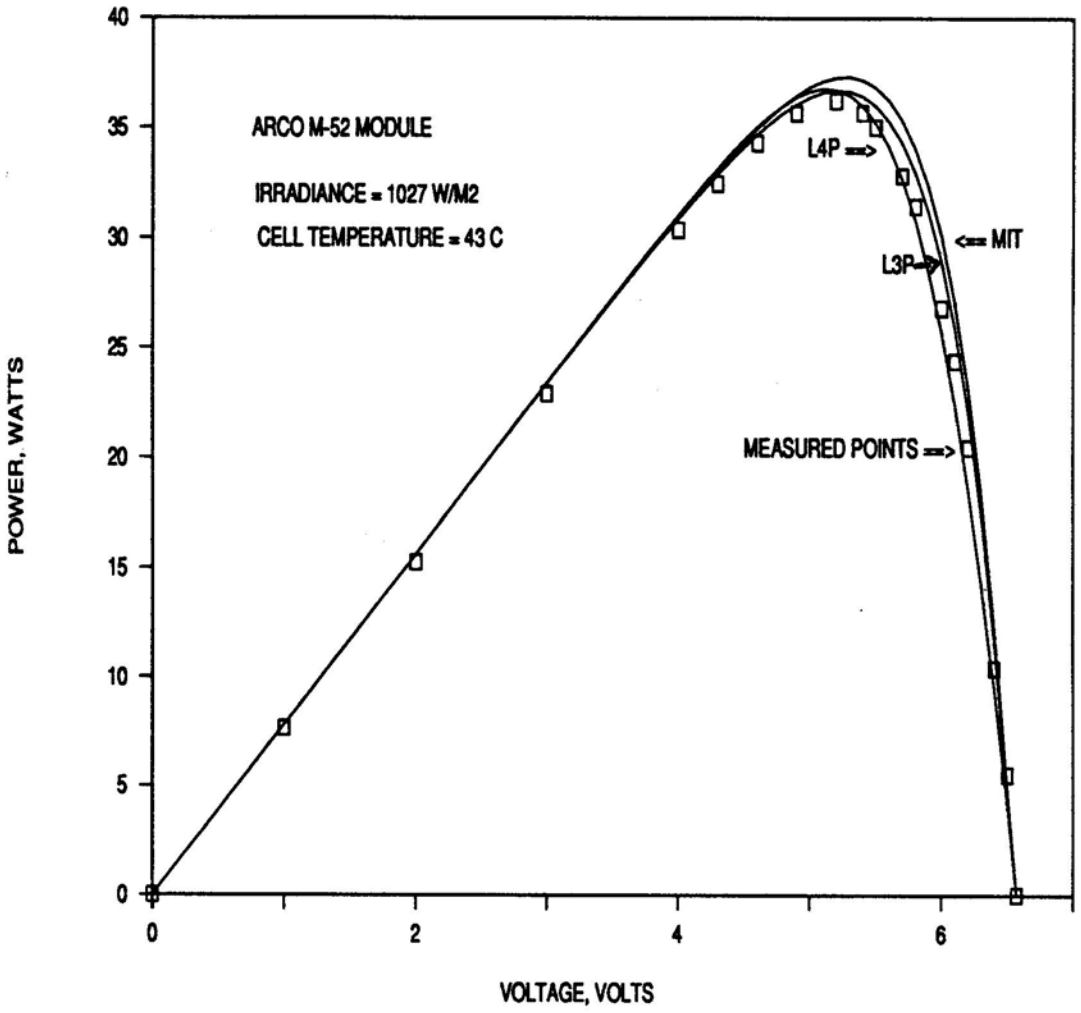

Figure 23a. ARCO Power- V Curves compared for L3P, lAP, and ~ Models

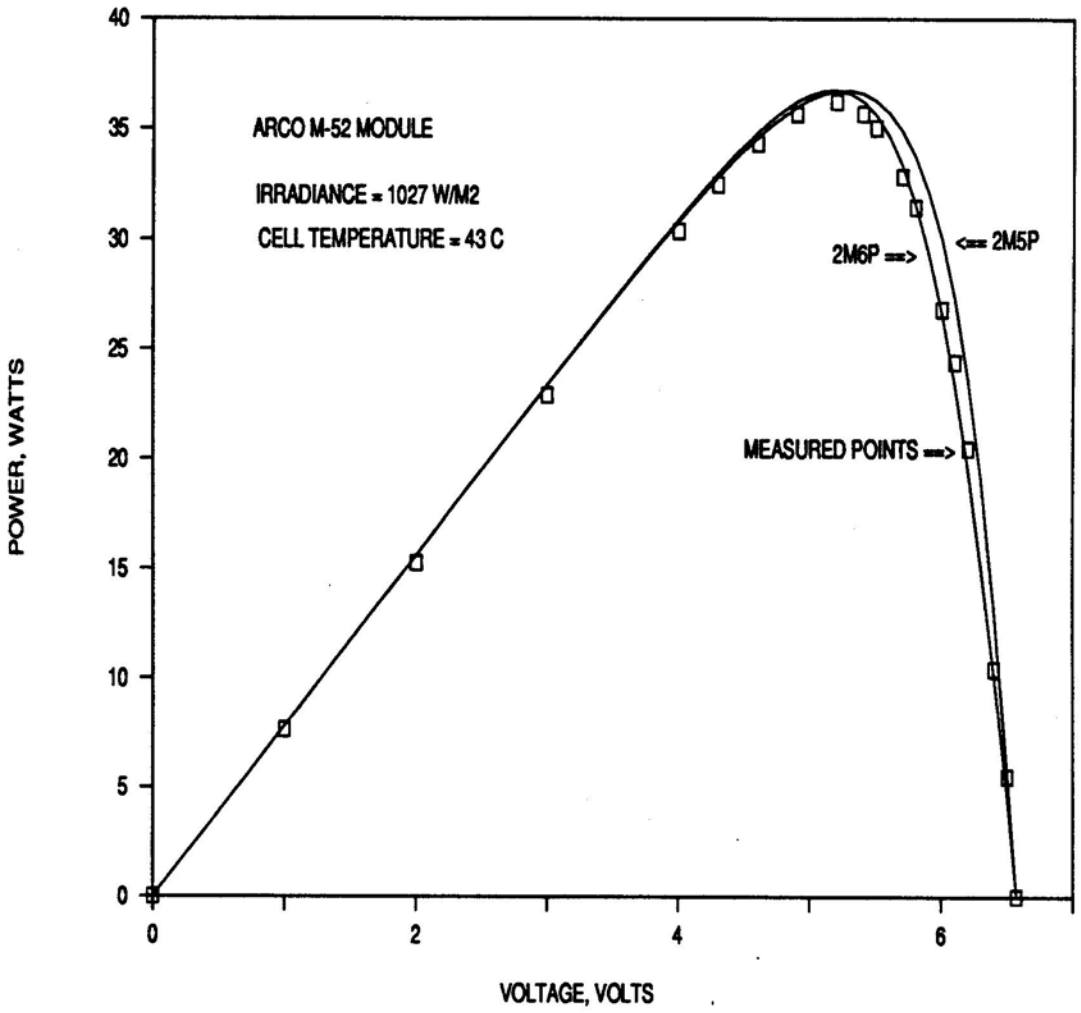

Figure 23b. ARCO Power- V Curves compared for 2M5P and 2M6P Models

Table 8. RMS % Power Differences, ARCO module

Irrad. = 1027 W/m^2, Cell Temp. = 43 °C	
I-V Model	RMS % Power Difference over full Power-V Curve
L3P	0.4
L4P	0.2
2M5P	0.4
2M6P	0.1
MIT	0.2

As with the Applied Solar Corp. module, the I-V models differ more at irradiance levels farther from the reference condition. Figures 24a and 24b show the translated I-V curves for the five models at a test condition of 510 W/m^2 and 43 °C. Measured values for the short circuit, open circuit, and maximum power points are shown. Figures 25a and 25b show the curves on a Power- V scale. The difference between the reported maximum power and predicted maximum power is about 5% for the L4P and MIT models, 6% for the 2M6P model, and 11 % for the L3P and 2M5P models. Each model underestimates the output, but the trend among models is consistent with the Applied Solar module results. For this module, the uniformly poor translations among each I-V model may be due to an inaccurate irradiance measurement at this test condition.

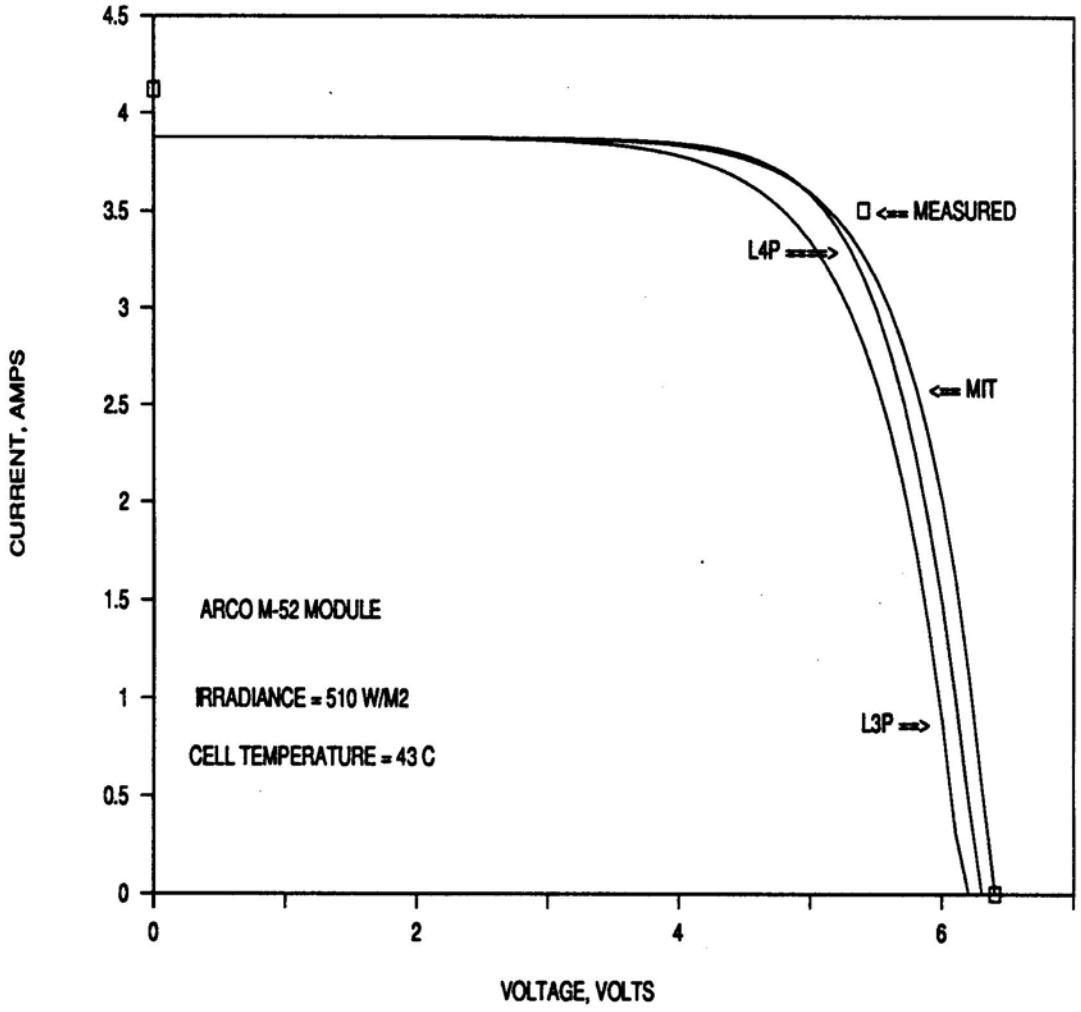

Figure 24a. ARCO I-V Curves for L3P. UP. and MIT Models at Low Irradiance

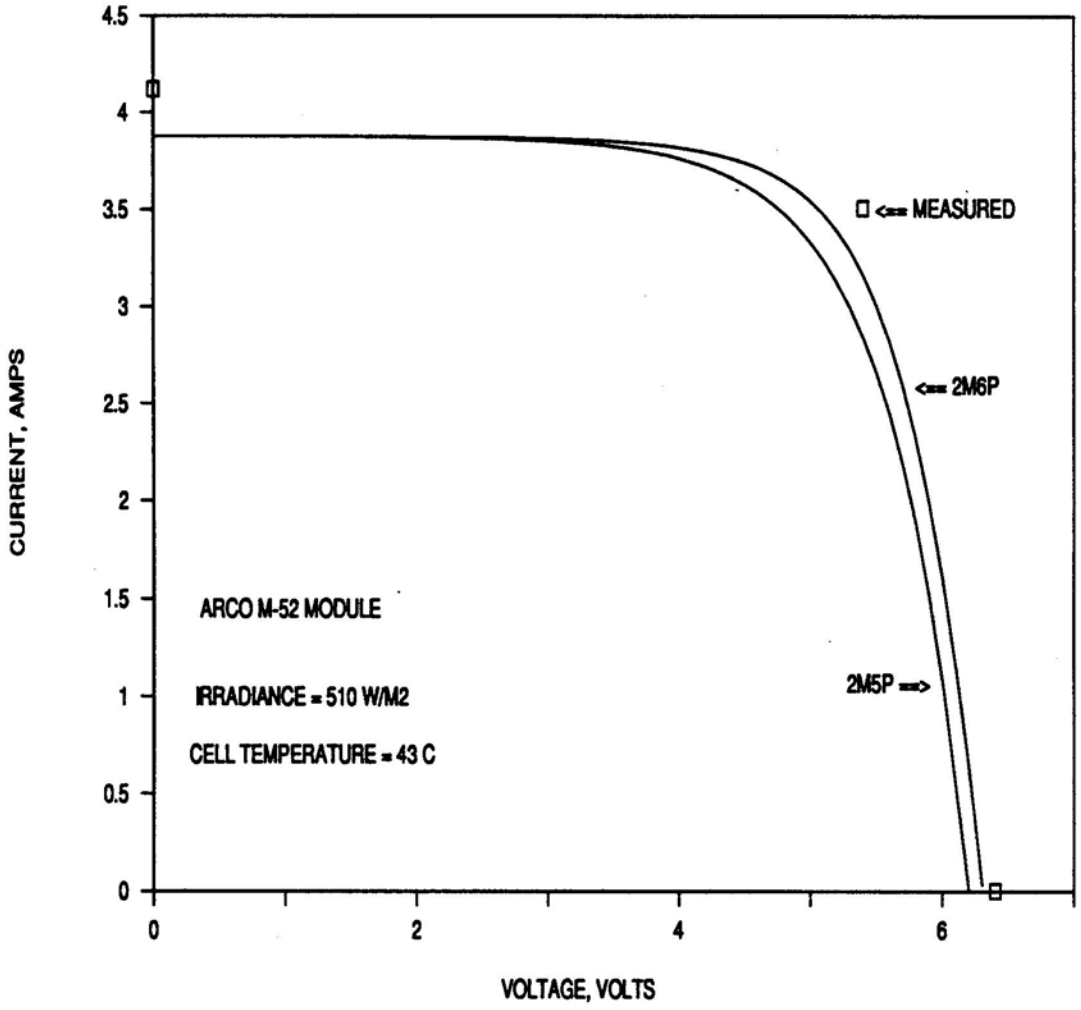

Figure 24b. ARCO I-V Curves for 2M5P and 2M6P Models at Low Irradiance

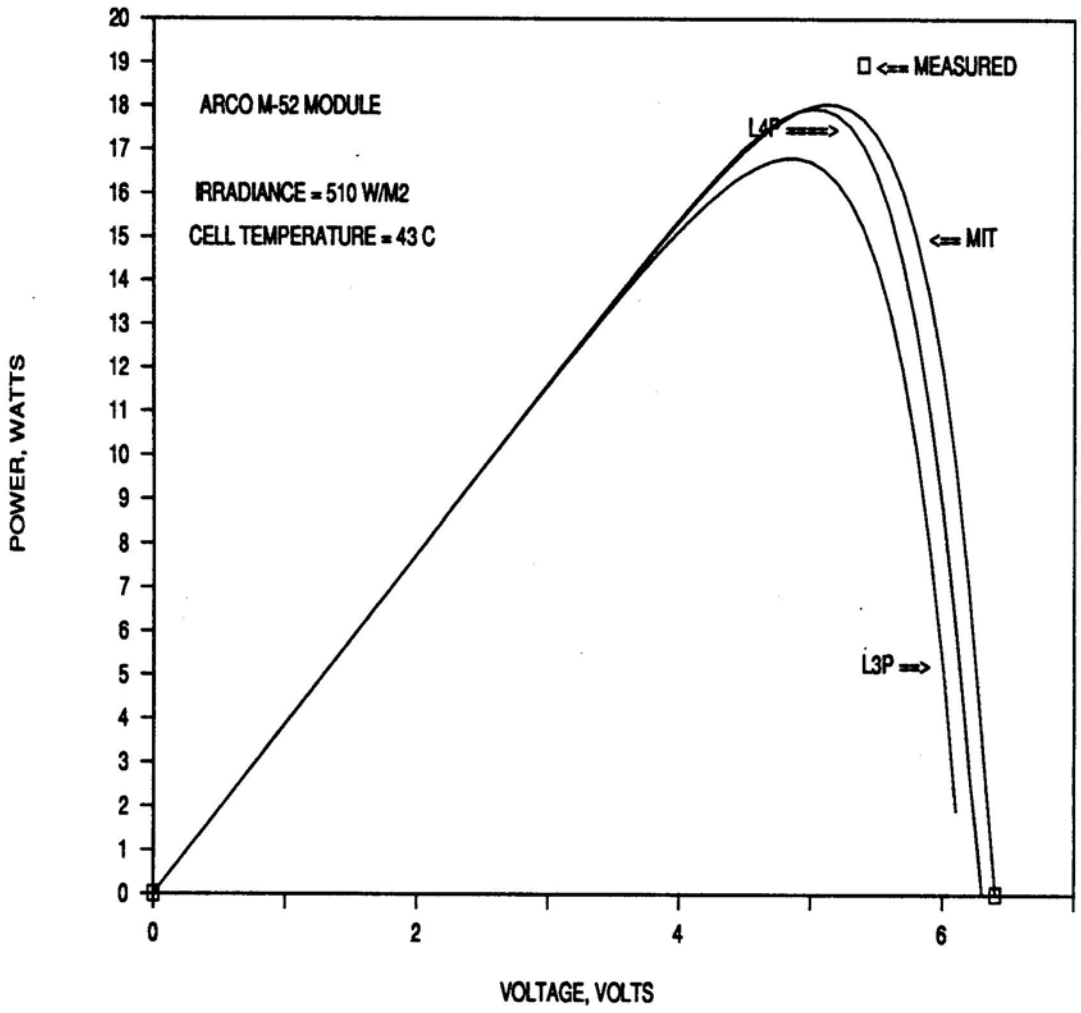

Figure 25a. ARCO Power- V Curves for L3P. lAP. and MIT Models at Low Irradiance

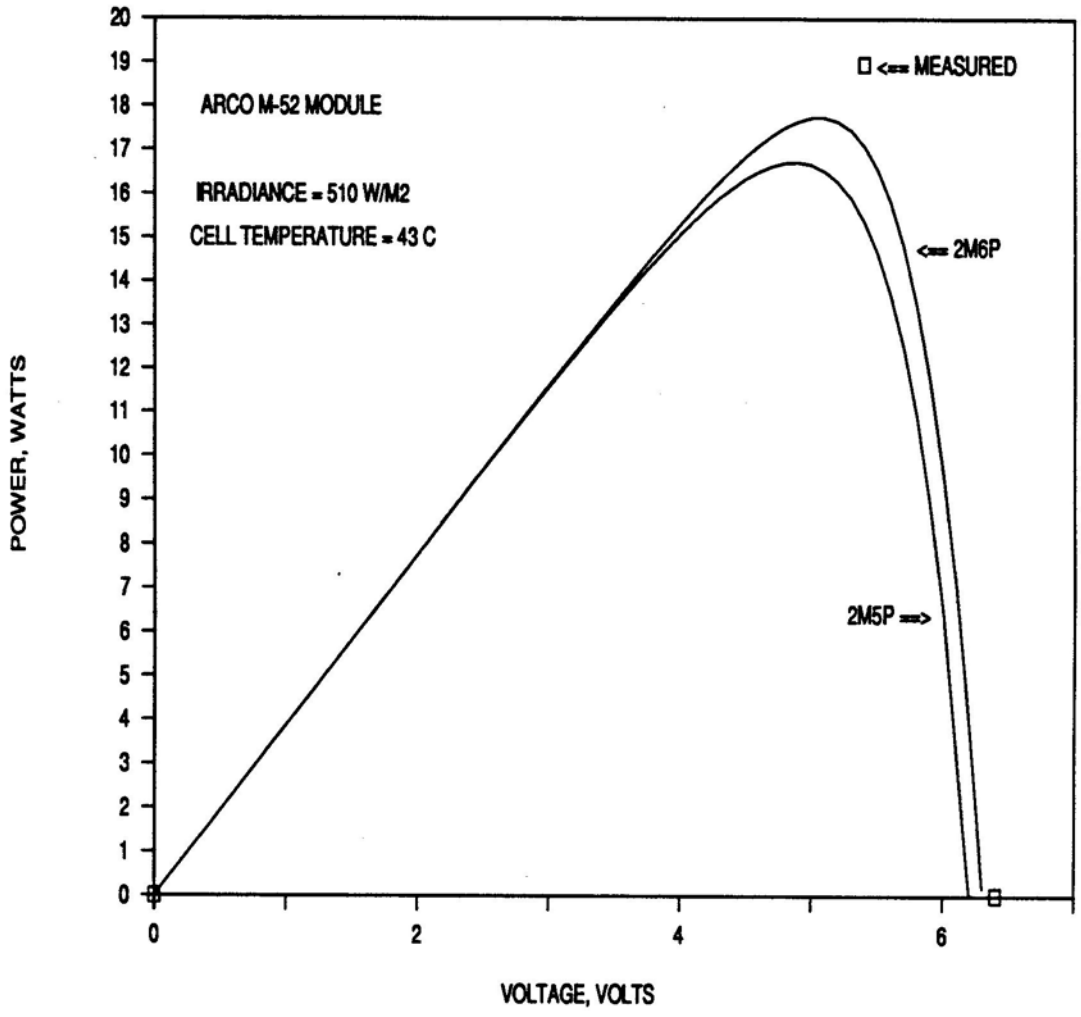

Figure 25b. ARCO Power- V Curves for 2M5P and 2M6P Models at Low Irradiance

The effect of varying cell temperature has a similar effect on I-V curves generated by each model, except for the MIT model. This is demonstrated in Figure 26, using the ARCO module. The irradiance is at the reference level, 1034 W/m^2. For this example, the cell temperature is 70 °C, and the reference cell temperature is 34 °C. At the reference condition, the I-V curves generated by all of the models are very similar, but at the higher cell temperature, the MIT model shows a clearly different response. The MIT model

predicts a maximum power that is 6 to 7% greater than that predicted by any of the other models. No actual test data were available at this condition.

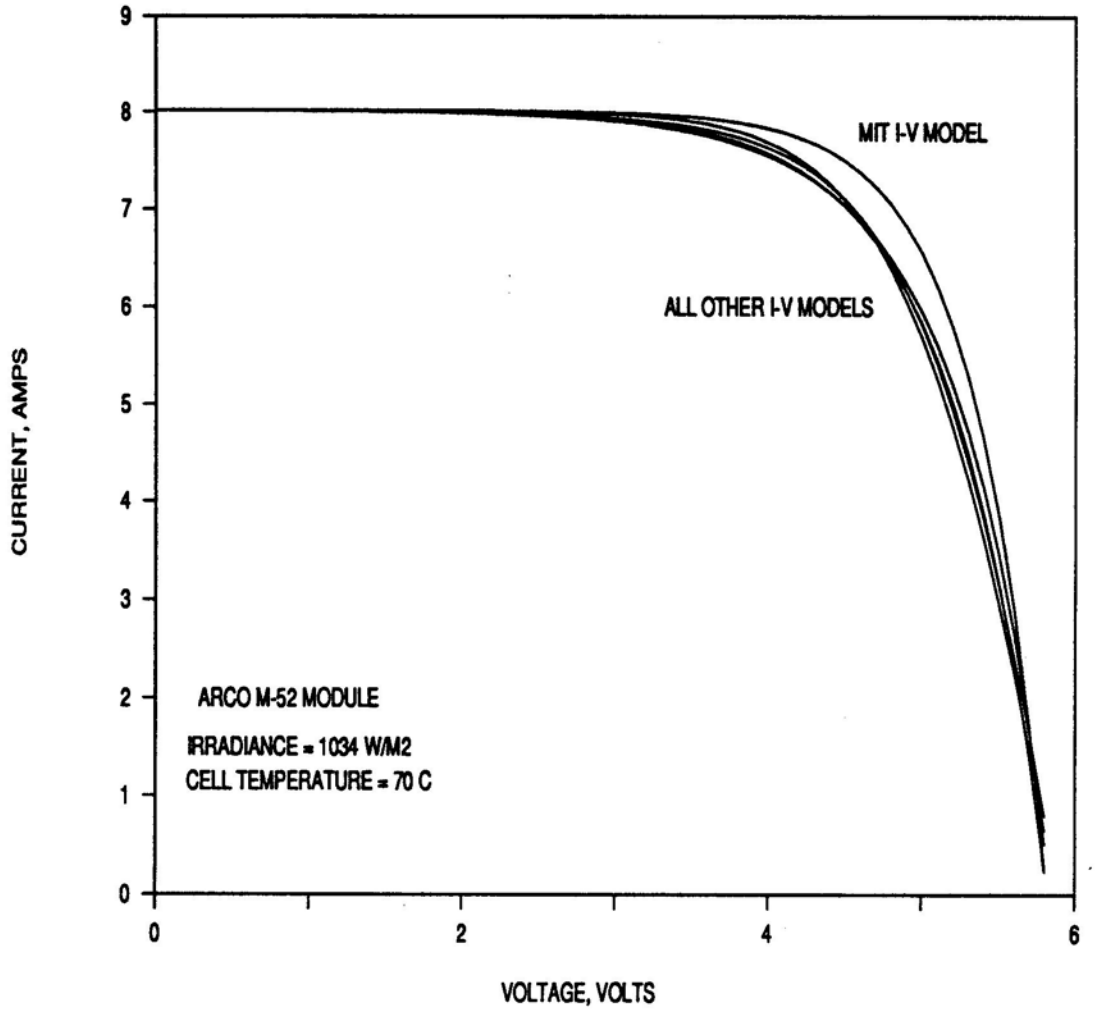

Figure 26. I-V Curves at High Cell Temperature

To check which model(s) translate I-V curves more accurately under varying cell temperatures, each was compared at several conditions where actual test data were available, that is, at constant irradiance but different cell temperatures. An example is shown in Figures 27a-d for the ARCO module, where the UP model is compared to one of the other models in each figure. The irradiance is about 910 W/m^2 at both cell temperatures of 42 °C and 58 °C. Part of the between-model variation seen is these figures is caused by a 10% decrease in irradiance from the reference level. The conclusion from Figure 26 and Figures 27a-d is that the MIT model does not translate as accurately as the other models for changes in cell temperature alone.

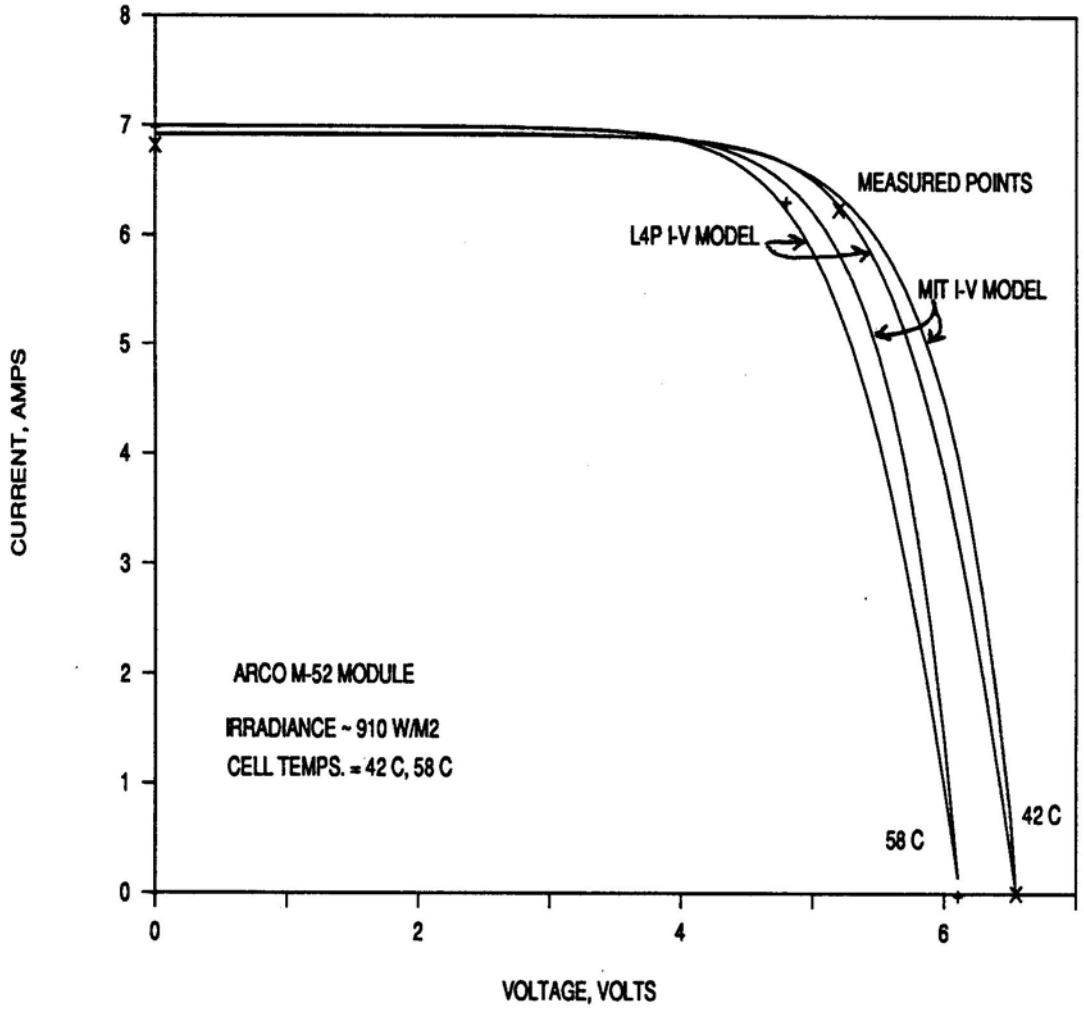

Figure 27a. I-V Curves for L4P and MIT Models at Two Temperatures

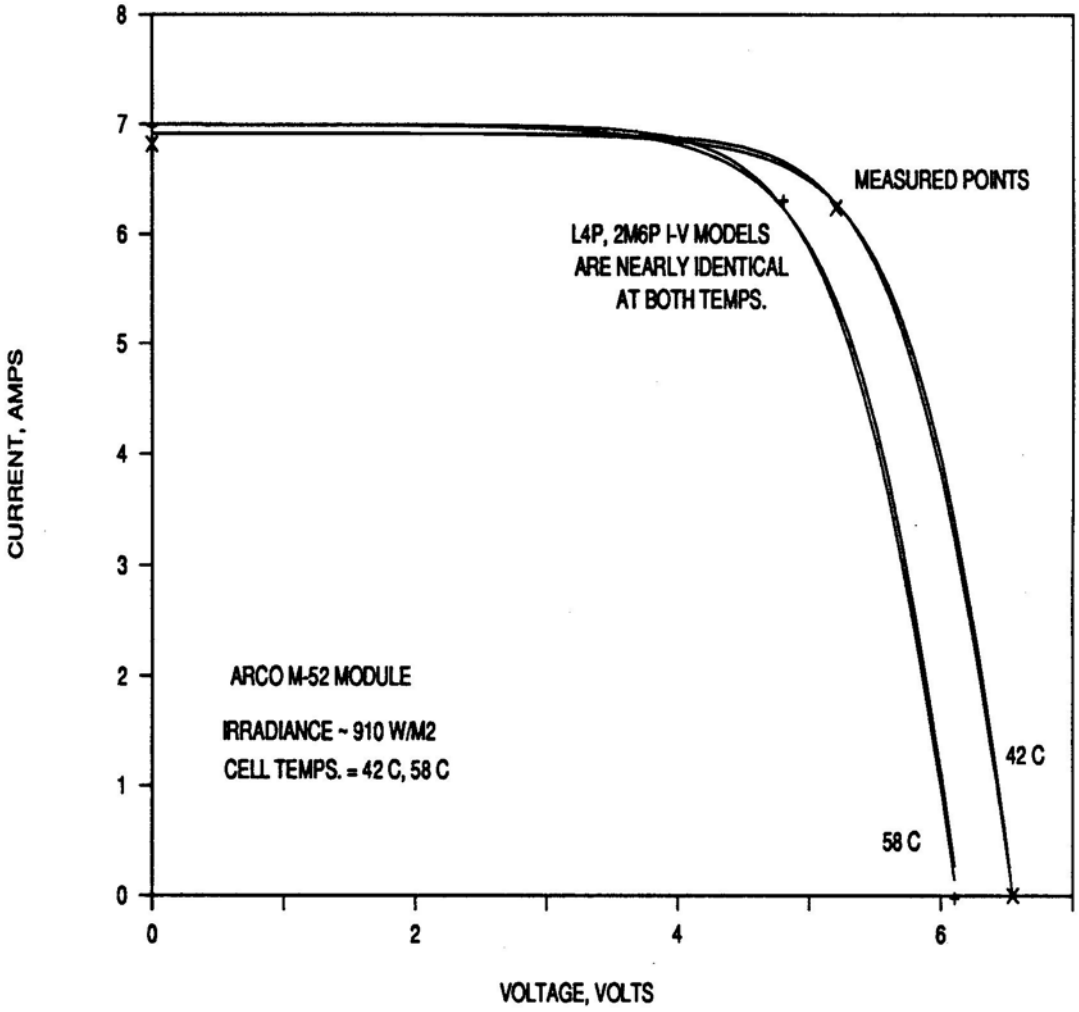

Figure 27b. I-V Curves for L4P and 2M6P Models at Two Temperatures

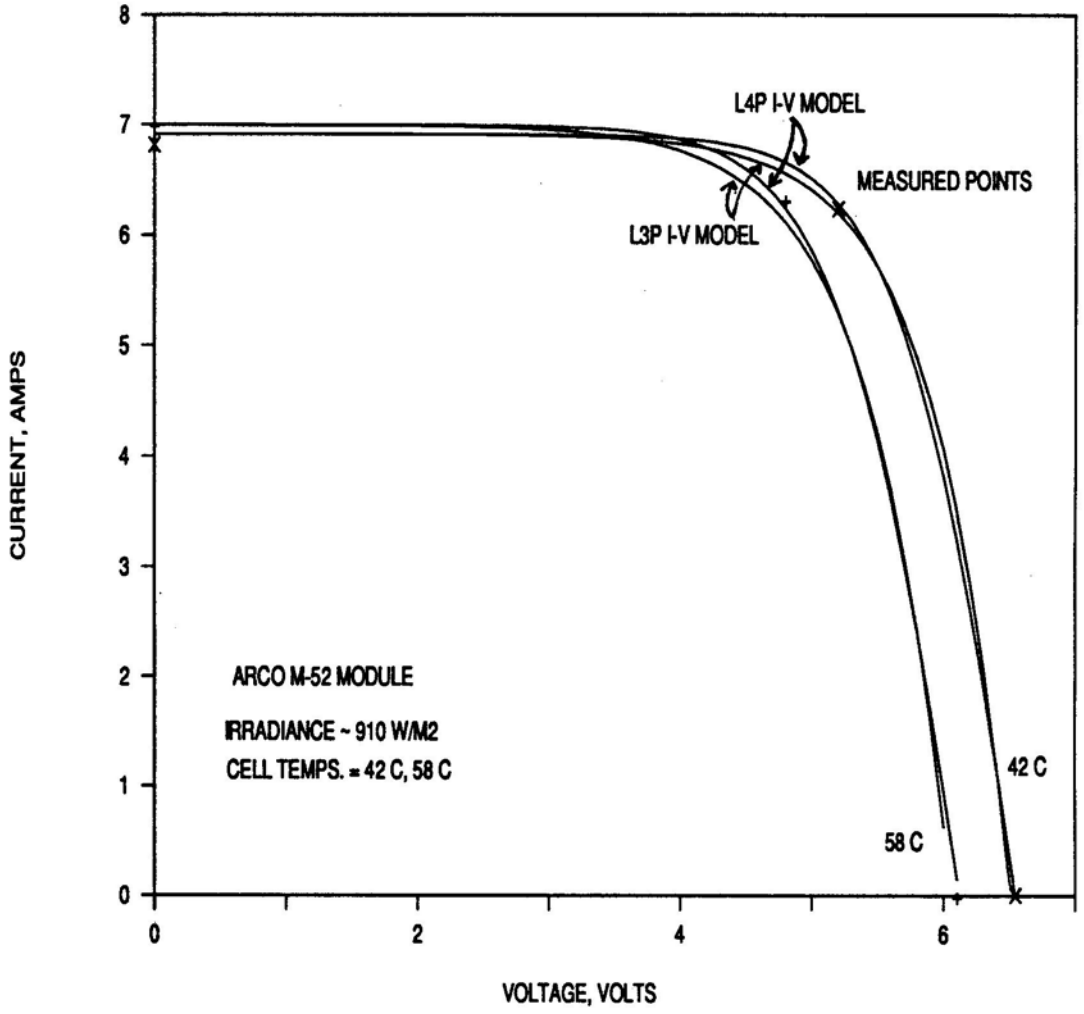

Figure 27c. I-V Curves for L4P and L3P Models at Two Temperatures

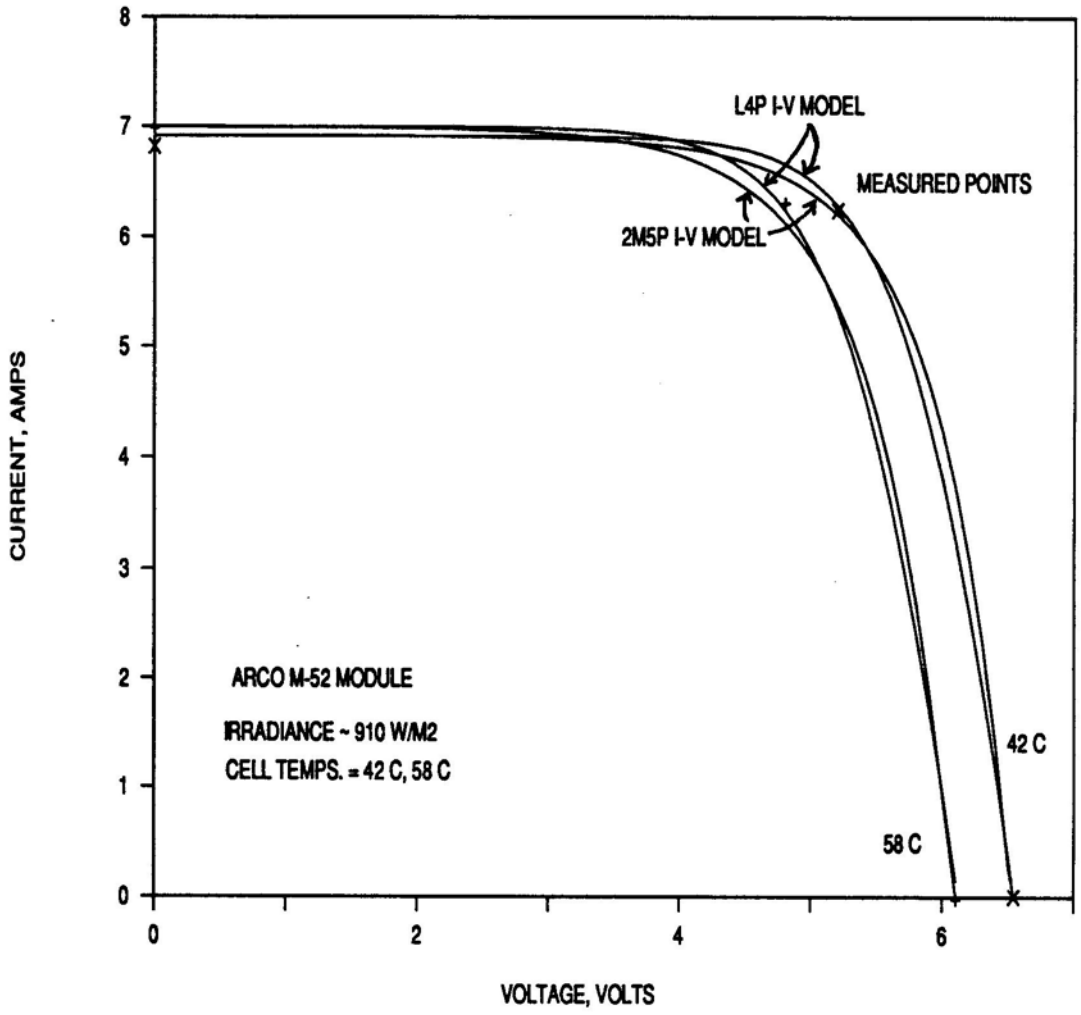

Figure 27d I-V Curves for lAP and 2M5P Models at Two Temperatures

Some conclusions from examining the I-V and Power-V curves for the five I-V models are that:

- Each model generates very similar I-V curves at the same reference condition.
- I-V Models which include a series resistance parameter (MIT, L4P, and 2M6P) are better predictors of I-V characteristics at irradiance levels away from the

reference level than the I-V models which ignore series resistance (L3P and 2M5P).

- The MIT model does not translate I-V curves as well as the other models for cell temperatures away from the reference cell temperature.
- Overall, I-V curves generated by the L4P and 2M6P models are the accurate and are practically indistinguishable from one another.

A related conclusion is that the increased accuracy demonstrated by the L4P and 2M6P models is obtained at the expense of added computational complexity. For the L3P, 2M5P, and MIT models, the Current may be calculated directly as a function of voltage. For both the L4P and 2M6P models, the current is an implicit function of voltage, so additional steps are necessary to converge on a proper I-V pair. The 2M6P model I-V equation (Eqn. 2.17) is algebraically more complex than the L4P model (Eqns. 2.24 or 2.67) because it contains an additional diode current term.

2.8.2 Maximum Power Point Evaluation

A well-designed direct-coupled PV system matches the PV array and its load so that the time-varying operating point is as close as possible to the time-varying maximum power point, especially during peak solar radiation periods. At a minimum, an I-V model must be able to reliably predict the I-V coordinates of the maximum power point over the system's expected range of irradiances and cell temperatures. However, the region of the I-V curve near the maximum power point at off-reference conditions is generally where all simplified I-V models are the least accurate. Therefore, comparing predicted

maximum power versus measured maximum power over a wide range of operating conditions provides a stringent test of an I-V model's accuracy.

In this section, a wide range of measured maximum power point data for three systems are compared to predicted maximum power output for six models. Five of these are the I-V curve models compared in the previous section and the sixth is the linear maximum power-only model discussed in Section 2.3.3.6. The linear model is included for comparison because it widely used among the performance models listed in Chapter 1 and has demonstrated good accuracy in validation tests on existing systems [21].

One of the three systems evaluated in this section is a large 4500 W array of Tri-Solar Corp. modules located at the Southwest Regional Experiment Station (SWRES) in Las Cruces, New Mexico. The other two are the 75 W Applied Solar and 43 W ARCO modules located at the Pacific Gas and Electric Co.'s San Ramon, California test site. 35 observations are included in the comparison for the Tri-Solar array, 98 for the Applied Solar module, and 86 for the ARCO module. The test conditions for these observations range from 79 to 1125 W/m^2 irradiance and from 18 to 65 °C cell temperature.

For each module, the percentage difference between the measured and predicted maximum power at each test condition (observation) is computed. This computation is done for each of the six models. The results for each system are shown in Figures 28 - 30 as a frequency distribution. The distribution is based on groups of observations whose

percentage error falls within bins of 5% width. A perfect model would demonstrate a single tall spike, centered at 0% error.

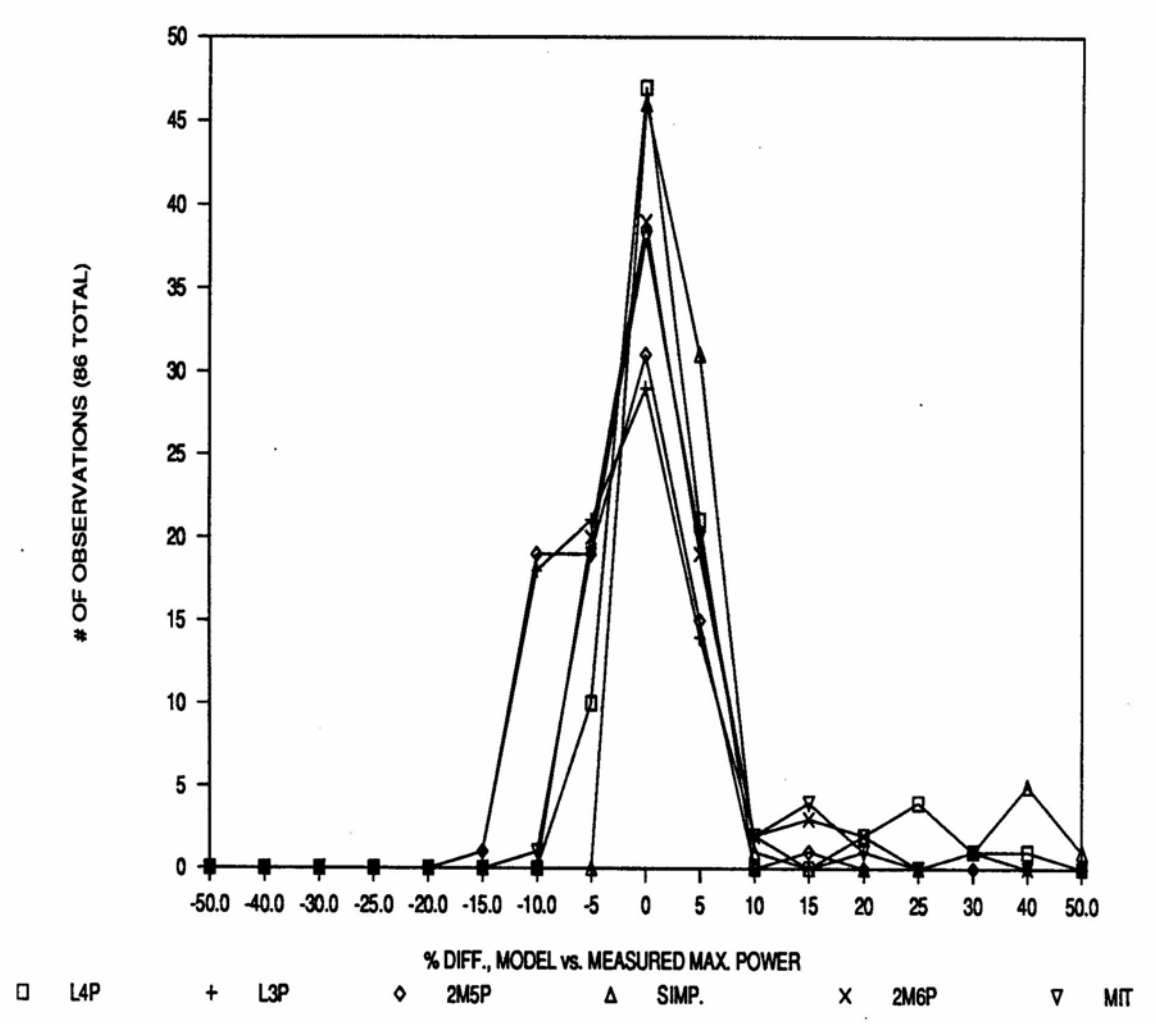

Figure 28. ARCO module: % Maximum Power Point Difference Compared for 6 Models

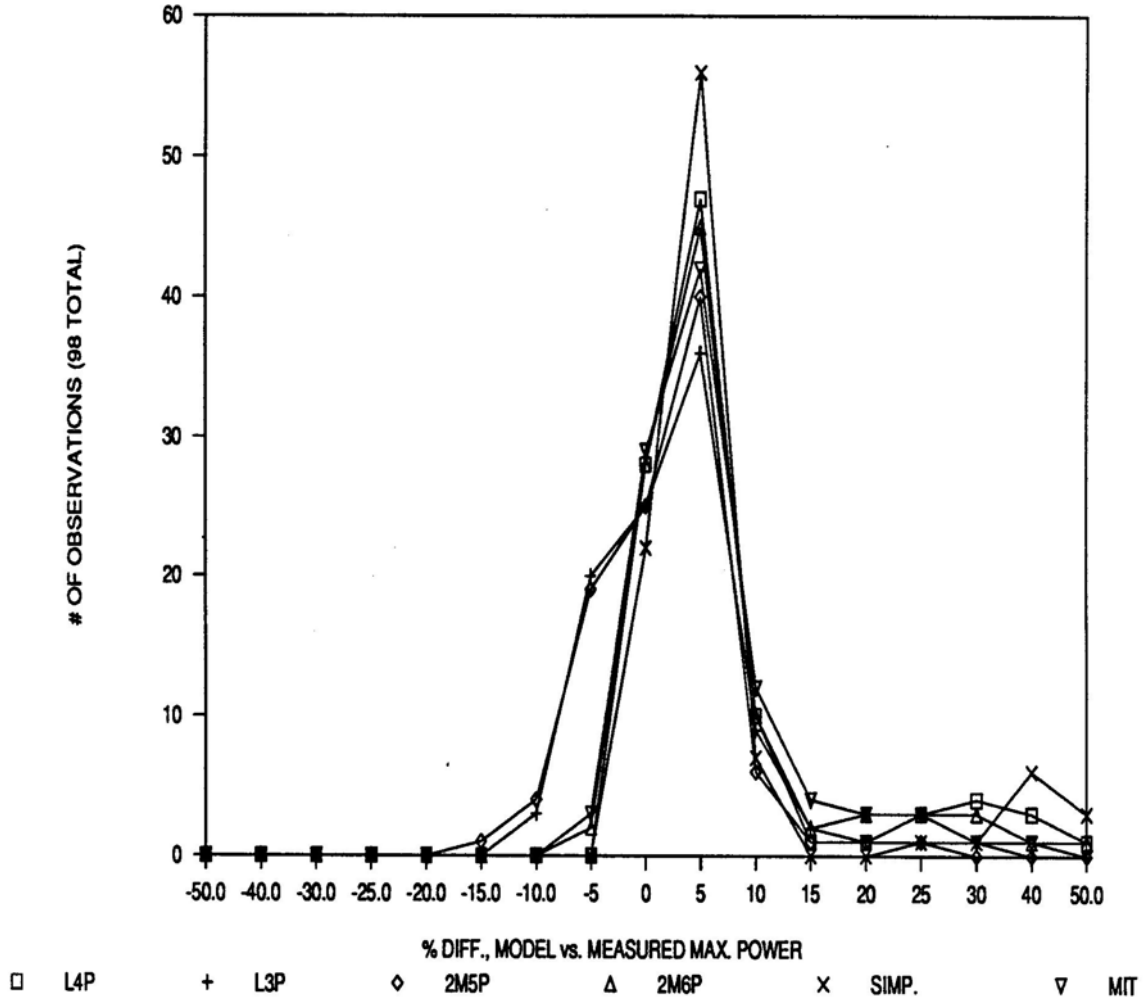

Figure 29. Applied Solar module: % Maximum Power Point Difference Compared for 6 Models

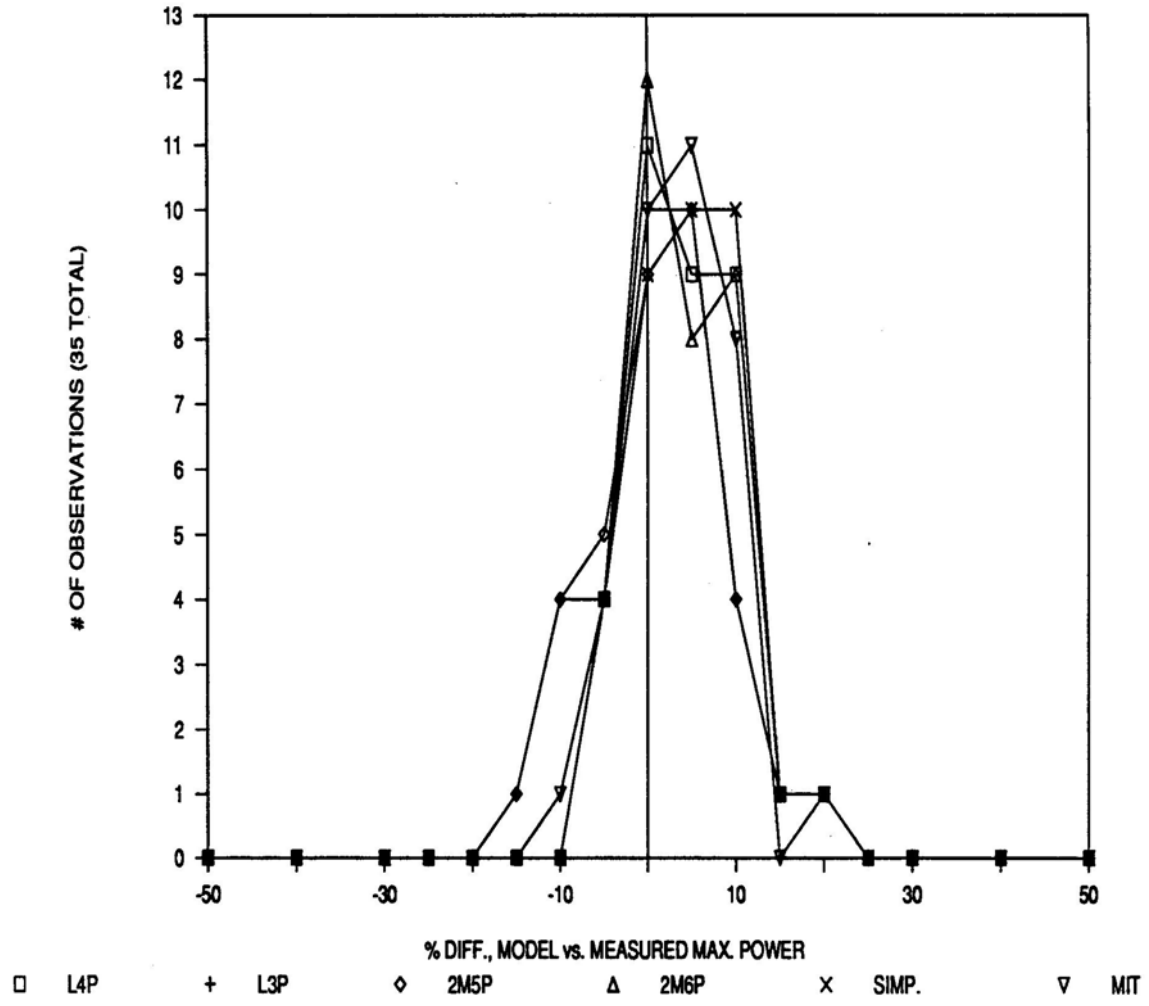

Figure 30. Tri-Solar Array: % Maximum Power Point Difference Compared for 6 Models

Several trends are evident in these figures. The frequency distribution for the linear model is narrower, more peaked, and centered closer to zero than for the other models. Approximately 75% of all observations for these models fall within ± 5% of the measured maximum power, and about 90% of the observations predict the maximum power within ± 10%. The L4P and 2M6P models are slightly less accurate than the linear model, followed by the MIT model. The distribution shapes for the L3P and 2M5P

models are shorter and wider than for the other models, but about 90% of the observations for these models still fall within ± 15% of the measured maximum power.

There are a small number of observations for the ARCO and Applied Solar modules that have a large percentage difference between the predicted and measured maximum power. Each of these observations were made at a reported irradiance of less than 125 W/m^2, typical of very early or very late observations at high incidence angles. Pyranometer accuracy is poor at high incidence angles and is a likely cause of error. Even if the reported irradiances were correct, large model differences at low irradiances are of lesser importance because the potential electric output under such conditions is small. All of the observations for the Tri-Solar array were made at irradiances of at least 316 W/m2 and all of the predicted values are within - 20 to + 15% of the measured maximum power.

The differences between measured and predicted values for all of the models are centered close to zero for the ARCO module and close to + 5% for the other systems. A possible reason why the results would be centered greater than zero is that the reported irradiance values are not modified to account for incidence angle effects. If the observations were distributed evenly over each day, an average incidence angle modifier would decrease the estimated output by about 5%. The ARCO results do not show the same skewed behavior, but this may actually be a compensating error caused by an inaccurate (overstated) reference condition.

Table 9 lists the % RMS difference and % mean bias difference averaged over all observations for each system. Equation 2.92 is used to compute the RMS statistic and the % mean bias difference is calculated with Eqn. 2.93:

$$\text{MEAN BIAS \% DIFF.} = \sum\left(P_{MAX,PRED.} - P_{MAX,MEAS.}\right)\times\frac{100}{AVG.P_{MAX,MEAS.}} \qquad (2.93)$$

Table 9. Statistical % Diff., Predicted vs. Measured Maximum Power for 6 Models

System-> Model	ARCO		Tri-Solar		Applied Solar	
	% Mean Bias Diff.	% RMS Diff.	% Mean Bias Diff.	% RMS Diff.	% Mean Bias Diff.	% RMS Diff.
L3P	-4.4	5.8	-0.4	6.4	-0.2	3.9
L4P	-1.4	3.1	2.3	5.8	2.2	3.7
2M5P	-4.6	6.0	-0.5	6.5	-0.3	4.2
2M6P	-1.9	3.5	1.9	5.7	2.1	3.7
MIT	-1.7	3.4	1.7	5.9	1.9	3.9
Linear	.1	2.6	2.6	5.9	2.0	3.4

These statistics confirm the general observations made from Figures 28 - 30. Averaged over all three systems, the UP model has the lowest % RMS difference of the five I-V models, 4.2%. The 2M6P and MIT models are slightly higher at 4.3% and 4.4%, respectively. The average % RMS difference for the Linear model is the lowest of all models, at 4.0%.

The % mean bias differences alone are misleading because a more erratic model may average out to a low mean bias difference, as is evident from Figures 28 - 30.

Therefore, the low bias differences for some systems for the L3P and 2M5P models are not good indicators of the model's accuracy. Averaged over all three systems, the mean bias differences are about 1 % for each of the L4P, 2M6P, MIT, and Linear models, so this statistic does not show any relative advantage among these models.

The overall conclusion from the maximum power point evaluation is that the L4P I-V model provides the best match with experimental data and also with an established theoretical model (Linear model). The average difference between the predicted and measured power is within the same ± 5% range of uncertainty typical of the irradiance measurements themselves. The L4P I-V model is a key element of the long-term direct-coupled performance model described in the following chapters.

The 2M6P model is nearly as accurate as the L4P model, but is computationally more complex. The MIT model is slightly less accurate than the L4P and 2M6P models and is computationally simpler, but as demonstrated in the previous section, is less accurate at cell temperatures far from the reference condition. For this evaluation, test data were available to select a reference cell temperature close to the normal operating temperature. Ordinarily, the designer is only provided test data at standard test conditions, in which case the reference cell temperature would be about 20 °C lower than normal operating cell temperatures.

2.9 Summary

In this chapter, fundamental PV electrical characteristics and equivalent circuits were described. Mathematical models of varying complexity were discussed, as well as criteria for selecting an appropriately detailed model. Solution methods for determining unknown parameters in current-voltage equations were developed, and the influence of variables such as irradiance, cell temperature, and electrical configuration were addressed. Finally, five I-V models were evaluated for use in an overall method to estimate the long-term performance of direct-coupled PV systems. The lumped, four parameter (or L4P) model was selected because it provided the best match with experimental data.